



# Origin and fate of hydrothermal fluids at Piton des Neiges volcano (Réunion Island): A geochemical and isotopic (O, H, C, Sr, Li, Cl) study of thermal springs

Bhavani Bénard, Vincent Famin, Pierre Agrinier, Bertrand Aunay, Geneviève Lebeau, Bernard Sanjuan, Francoise Vimeux, Gérard Bardoux, Chrystel Dezayes

## ► To cite this version:

Bhavani Bénard, Vincent Famin, Pierre Agrinier, Bertrand Aunay, Geneviève Lebeau, et al.. Origin and fate of hydrothermal fluids at Piton des Neiges volcano (Réunion Island): A geochemical and isotopic (O, H, C, Sr, Li, Cl) study of thermal springs. *Journal of Volcanology and Geothermal Research*, 2020, 392, pp.106682. 10.1016/j.jvolgeores.2019.106682 . hal-02538144

HAL Id: hal-02538144

<https://brgm.hal.science/hal-02538144>

Submitted on 21 Jul 2022

**HAL** is a multi-disciplinary open access archive for the deposit and dissemination of scientific research documents, whether they are published or not. The documents may come from teaching and research institutions in France or abroad, or from public or private research centers.

L'archive ouverte pluridisciplinaire **HAL**, est destinée au dépôt et à la diffusion de documents scientifiques de niveau recherche, publiés ou non, émanant des établissements d'enseignement et de recherche français ou étrangers, des laboratoires publics ou privés.



Distributed under a Creative Commons Attribution - NonCommercial 4.0 International License

1      Origin and fate of hydrothermal fluids at Piton des Neiges volcano (Réunion  
2      Island): a geochemical and isotopic (O, H, C, Sr, Li, Cl) study of thermal springs

3      Bhavani Bénard<sup>ab</sup> (corresponding author), Vincent Famin<sup>a</sup>, Pierre Agrinier<sup>c</sup>, Bertrand Aunay<sup>b</sup>,  
4      Geneviève Lebeau<sup>a</sup>, Bernard Sanjuan<sup>d</sup>, Françoise Vimeux<sup>e</sup>, Gérard Bardoux<sup>c</sup>, Chrystel Dezayes<sup>d</sup>

5      <sup>a</sup> Laboratoire GéoSciences Réunion, Université de La Réunion, Institut de Physique du Globe de  
6      Paris, Sorbonne Paris Cité, Université Paris Diderot, UMR 7154 CNRS, F-97744 Saint Denis, La  
7      Réunion

8      <sup>b</sup> BRGM, F-97417 Saint-Denis de La Réunion, France

9      <sup>c</sup> Institut de Physique du Globe de Paris, Université Sorbonne Paris Cité, Université Paris Diderot,  
10     CNRS, UMR 7154, 75005, Paris, France

11     <sup>d</sup> BRGM, F-45060 Orléans, France

12     <sup>e</sup> Institut de Recherche pour le Développement, Laboratoire HydroSciences Montpellier (UMR  
13     5569) et Laboratoire des Sciences du Climat et de l'Environnement (UMR 8212), CEA Saclay,  
14     Orme des Merisiers, 91191 Gif-sur-Yvette Cedex, France

15

16     Contacts: bhavani.benard@univ-reunion.fr, vincent.famin@univ-reunion.fr, agrinier@ipgp.fr,  
17     b.aunay@brgm.fr, genevieve.lebeau@univ-reunion.fr, b.sanjuan@brgm.fr,  
18     [francoise.vimeux@lsce.ipsl.fr](mailto:francoise.vimeux@lsce.ipsl.fr), bardoux@ipgp.fr, c.dezayes@brgm.fr

19     Declarations of interest: none

20     **Abstract**

21     As many ocean basaltic volcanoes worldwide, Piton des Neiges (Réunion Island) hosts a  
22     hydrothermal system that represents a potential geothermal resource. Despite several  
23     prospection campaigns over the past decades, this potential has never been confirmed because  
24     many aspects of fluid supply and circulation remain unclear. To track the origin and fate of  
25     hydrothermal fluids, we analyzed the geochemistry of thermal springs (water and gas), by  
26     combining conventional tracers (major-trace elements and O, H, C, Sr, Li isotopes) with Cl

27 isotopes, a geochemical tool under development. Added to literature data, our new results allow  
28 us to compare the composition of thermal springs with cold waters, rocks, gas, and fumarolic  
29 deposits from La Réunion and elsewhere, and to untwine the complex history of fluid mixing that  
30 constitutes the geothermal system of Piton des Neiges.

31  $\delta^{18}\text{O}_{\text{H}_2\text{O}}$  and  $\delta\text{D}_{\text{H}_2\text{O}}$  values of springs (-8.67 to -4.9 and -56.3 to -23.5 ‰ VSMOW,  
32 respectively) are positioned close to the local meteoric water line, showing that thermal waters  
33 are of meteoric origin. However, their depletion in heavy isotopes relative to cold waters suggests  
34 a recharge strongly influenced by cyclones, with a possible contribution from high altitude ( $\geq$   
35 2000 m) rainfalls. Their absence of  $^{18}\text{O}$  enrichment relative to the local meteoric water line  
36 indicates that the isotopic exchange between rocks and water is very limited, and therefore  
37 suggests that their deep temperatures are relatively low and/or the water/rock ratios are high.  
38  $\delta^{13}\text{C}$  values in thermal waters (-8.0 to +3.2 ‰ PDB) and gases (-6.7 to -5.3 ‰ PDB) confirm  
39 that carbon is essentially of magmatic origin, which we interpret as supplied by regional  
40 degassing of La Réunion hotspot. Major-trace elements and  $^{87}\text{Sr}/^{86}\text{Sr}$  (0.704142 to 0.704336),  
41  $\delta^7\text{Li}$  (+2 ‰ and +34.8 ‰ LSVEC), and  $\delta^{37}\text{Cl}$  (-0.35 ‰ and +0.40 ‰ SMOC) compositions  
42 show that three additional processes contribute to the mineralization of thermal waters: 1)  
43 interaction with basalt at temperatures  $\geq 50$  °C, 2) very limited seawater contamination (< 3  
44 mol%), and/or 3) leaching of trachyte or scrubbing of fumarolic gas or condensates emitted by a  
45 shallow trachytic magma in the volcanic edifice.

46 The geothermal system of Piton des Neiges is thus the result of meteoric water interaction  
47 with a trachytic heat source (as a solidified intrusion or a magma pocket), unrelated to the CO<sub>2</sub>  
48 flux. We also emphasize that thermal waters at Piton des Neiges are exceptionally isolated from  
49 seawater compared to other geothermal systems in ocean island volcanoes worldwide, which  
50 implies a heat source located above the seawater/freshwater interface. These inferences are of  
51 critical importance for the future geothermal exploration on the island, as they suggest that the  
52 geothermal resource is within reach of relatively shallow drilling depths ( $\leq 1000$  m).

53 **Keywords:** Piton des Neiges, Réunion Island; Ocean island volcano; Thermal springs;  
54 Hydrothermal system; Geothermal exploration; Major and trace elements; Isotope chemistry;  
55 Chlorine isotopes

## 56 **1. Introduction**

57 Ocean island basaltic volcanoes are among the most prized geological settings for geothermal  
58 exploitation, because they cumulate the advantages of a shallow and significant heat source,  
59 almost unlimited water supply, and low concentrations of toxic or radioactive elements in waters  
60 compared to granitic or andesitic settings. Iceland, São Miguel (Azores), Big Island (Hawaii) and

61 Pantelleria (Italy) are emblematic examples of such basaltic islands being exploited or showing  
62 potential for geothermal energy (Bertani, 2005; Gianelli and Grassi, 2001). However, ocean island  
63 volcanoes are also renowned for the complexity of their geothermal systems, seldom matching  
64 the ideal case of a heat source/reservoir/cap rock superposition as in the model of Johnston et  
65 al., (1992). This complexity requires case-by-case studies of fluid sources and pathways, which  
66 often discourages geothermal prospection or exploitation.

67 The island of La Réunion illustrates this difficulty of evaluating the geothermal potential of  
68 ocean island basaltic volcanoes. Réunion Island is made of two edifices, Piton de la Fournaise  
69 which is among the most active volcanoes of the world, and Piton des Neiges presently in a  
70 dormant state since 12 to 29 ka (Delibrias et al., 1986; Deniel et al., 1992; Gillot and Nativel,  
71 1982). Piton des Neiges displays ample evidence of hydrothermal activity, including thermal  
72 springs (up to 50 °C for the hottest), fumarole deposits, and CO<sub>2</sub> – He – Rn anomalies (Marty et  
73 al., 1993; Rançon and Rocher, 1985; Sanjuan et al., 2001). Between 1980 and 2005, exploration  
74 campaigns of geophysics and drillings demonstrated the presence of dense intrusive complexes  
75 beneath Piton des Neiges, and temperature gradients locally exceeding 90 °C/km (see Dezayes  
76 et al., (2016) for a review). Using chemical and isotope geothermometers, geochemical studies  
77 also revealed the temperature of water-rock interaction ranged from 100 to 160°C for most of  
78 the thermal springs, (Lopoukhine and Stieltjes, 1978; Sanjuan et al., 2001). Despite these  
79 promising indicators, prospection did not fully succeed in locating and quantifying the resource of  
80 Piton des Neiges, partly because of the complex structure of this polygenic volcano, but most of  
81 all because of the difficulty of identifying multiple fluid reservoirs and pathways from the  
82 geochemical tools and data available at that time.

83 The objective of this paper is to improve our understanding of Piton des Neiges' hydrothermal  
84 system, by untangling the contribution of each fluid pool and the mixing and heating history of  
85 these fluids. The adopted strategy is to widen the geochemical description of thermal waters by  
86 applying proven and newly-developed tracers, and to increase the number of analyzed springs  
87 compared to previous studies. Our new results are combined with literature data into an  
88 exceptionally large geochemical set of major, trace elements and O, H, C, Sr, Li and Cl isotopes  
89 analyses of thermal springs from Piton des Neiges. Compared with the chemistry of rocks,  
90 seawater, cold waters, and fumarolic products from Réunion as well as from other similar  
91 geological contexts, this large dataset allows us to untwine the complex history of fluids at the  
92 origin of Piton des Neiges' hydrothermal system. The proposed circulation model may be used as  
93 a predictive tool for geothermal exploration in Réunion and other basaltic islands.

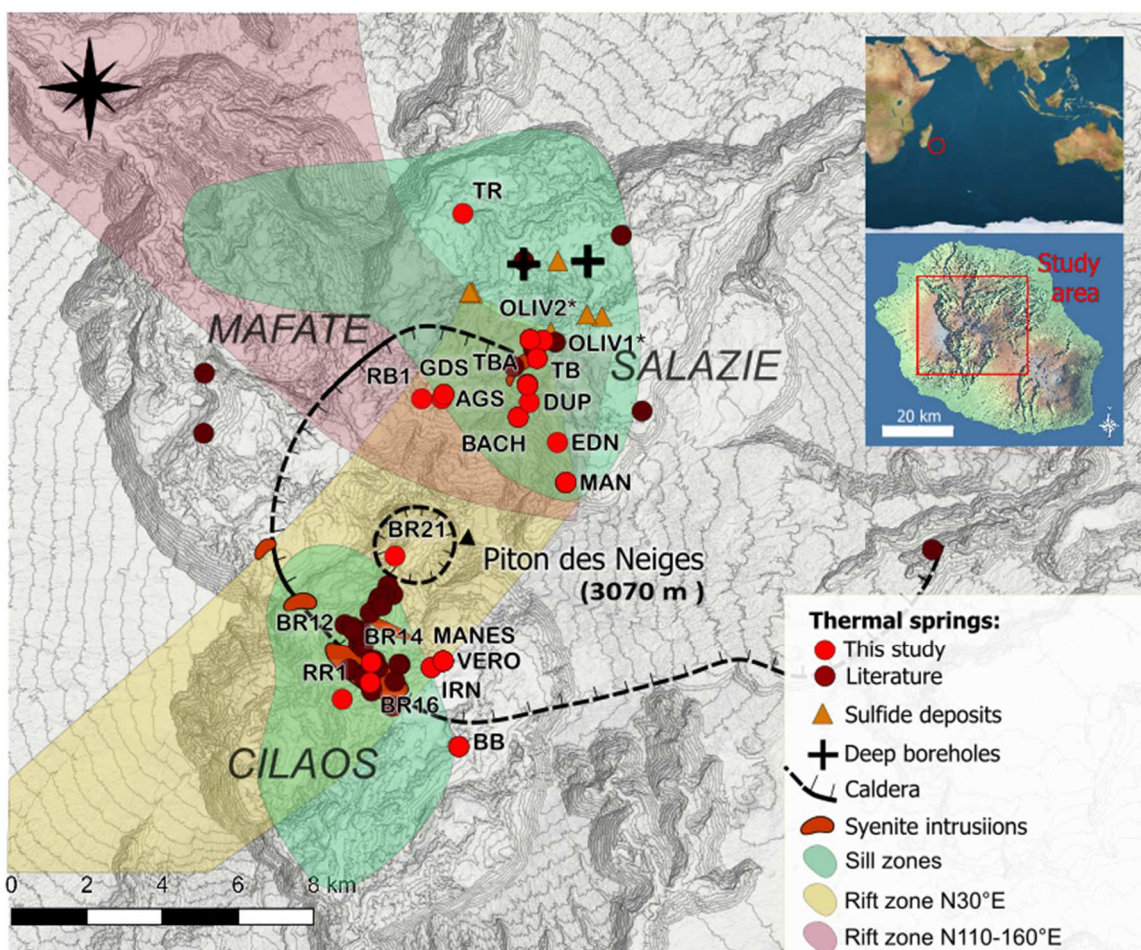
94 **2. Geological and hydrogeological settings**

95 Piton de la Fournaise and Piton des Neiges are often considered as analogue volcanoes with a  
96 similar structure and evolution, the former being in its shield building stage while the latter is at  
97 the end of its lifetime. Piton des Neiges is estimated to have emerged at ~3 Ma and has  
98 produced transitional basic magmas until 430 ka (Kluska, 1997; McDougall, 1971). After a 80 ka  
99 period of repose, the volcano entered into a differentiated stage 350 ka ago and produced alkali  
100 magmas ever since (Gillot and Nativel, 1982; Kluska, 1997). The terminal volcanism of Piton des  
101 Neiges began at about 210 ka, with the emission of highly differentiated magmas such as  
102 trachytes and syenites. The last known eruption of Piton des Neiges dates back to 12 ka (U/Th),  
103 22 ka ( $^{14}\text{C}$ ) or 29 ka (K/Ar), depending on the radiometric dating technique (Delibrias et al.,  
104 1986; Deniel et al., 1992; Gillot and Nativel, 1982).

105 Since its last activity, the heavy rainfalls under tropical climate have favored erosion of the  
106 volcanic edifice, now incised by three cirques (subcircular depressions), Salazie to the north,  
107 Mafate to the northwest, and Cilaos to the south (Figure 1). These deep cirques have dissected  
108 the inner structure of the volcano, erasing most of the surface evidence of calderas. Based on  
109 patchy observations of faults, offset lava layers, pyroclastic deposits or radial dykes, two calderas  
110 have been proposed: a large one running through the three cirques formed at the beginning of  
111 the terminal stage (210 – 180 ka), and a smaller one in the summit area of Piton des Neiges  
112 formed during its last activity (Figure 1). On the other hand, erosion has exposed the  
113 hypovolcanic complex, made of dense gabbroic plutons and basaltic, trachytic and syenitic planar  
114 intrusions. Planar intrusions are organized into two rift zones N030-40 and N120-160, and two sill  
115 zones between 800 and 1300 m above sea level (Chaput et al., 2017, 2014). Syenite intrusions,  
116 which consist in 30 – 100 m thick dykes in the cirques of Cilaos and Salazie, are of particular  
117 importance for the present study for two reasons: (1) they represent major dyke structures of  
118 the terminal volcanic activity, since they are located within the N030 rift zone, and are also  
119 interpreted to delineate the largest caldera at 210 – 180 ka (Chevalier, 1979; Rocher, 1988); (2)  
120 because many thermal springs are found in their vicinity, syenite dykes might be associated with  
121 the heat source of the hydrothermal system, or at least with the fracture network enabling fluid  
122 circulation.

123 The hypovolcanic complex of Piton des Neiges is also affected by several phases of low-grade  
124 metamorphism and hydrothermal alteration (Chevalier, 1979; Rançon, 1985), resulting in the  
125 secondary precipitation of phrenite-pumpellyite facies minerals in rocks of the shield-building  
126 stage, followed by carbonate precipitation in differentiated rocks as well as in basic rocks (Famin  
127 et al., 2016). This long history of construction and destruction, intrusive activity and secondary  
128 mineral precipitation strongly affects the hydrogeology of Piton des Neiges, by limiting the escape  
129 of freshwater toward the sea and its downward infiltration in the lowermost, oldest and most  
130 impermeable rock units (Join et al., 2005; Violette et al., 1997).

131 The tropical climate of Réunion Island consists in a dry season (April-November), and a wet  
 132 season (December-March) that delivers huge precipitation rates (annual average of  $\sim$  2500 mm  
 133 in the cirques). Most of these wet season rainfalls occur as cyclones (five events per year in  
 134 average for the period 1981 – 2010; Jumaux et al., 2011), providing ample meteoric water to  
 135 feed a hydrothermal system. However, the hydrothermal system of Piton des Neiges may be also  
 136 alimented by seawater, as in the case of many other volcanic islands (Adams, 1996; Arnórsson,  
 137 1995a, 1995b; Carvalho et al., 2006; Druecker and Fan, 1976; Thomas, 1984). To date, no  
 138 hydrogeological model explicitly accounts for the recharge of the deep thermal aquifers, and the  
 139 relative contribution of seawater and meteoric water to the hydrothermal system remains to be  
 140 evaluated.



141  
 142 Figure 1: Location of thermal springs in Piton des Neiges, Réunion Island. Springs sampled for this study are  
 143 labeled. Sulfide deposits (Lopoukhine and Stieljes, 1978; Rançon and Rocher, 1985), proposed calderas  
 144 (Chevalier, 1979), syenite intrusions, and rift and sill zones (Chaput et al., 2017) are also represented. Most  
 145 springs are located in the cirques of Salazie and Cilaos. Map in UTM coordinates (EPSG:2975, RGR92 / UTM 40s,  
 146 relief contours at 100 m intervals) from RGE ALTI® - IGN.

147 **3. Methods**

148 Thermal springs were sampled during two campaigns, the first one in June 2015 and the  
149 second one from December 2015 to January 2018. These campaigns yielded a total of twenty-  
150 seven water samples and seven gas samples of eighteen springs, to be analyzed for major, trace  
151 elements and O, H, Sr, Li, Cl and/or C isotopes (See Table B.1 for coordinates). Additionally,  
152 sixteen archive spring and river samples from Sanjuan et al. (2001) were analyzed for Li  
153 concentration,  $\delta^7\text{Li}$  and  $\delta^{37}\text{Cl}$ . During each sampling, the pH, temperature, and electrical  
154 conductivity (EC) of water were measured at the spring outlet. pH and EC are expressed at the *in*  
155 *situ* water temperature. For major, trace elements and Sr, Li, Cl isotope analyses, water samples  
156 were collected in HDPE bottles after filtration at 0.2  $\mu\text{m}$  on site. For O and H isotope analyses,  
157 water was mainly sampled in amber glass bottles with cone shaped caps to avoid any isotopic  
158 exchange with ambient air, except during the first campaign (HDPE bottles). During the second  
159 campaign, water samples were also collected for analysis of total dissolved inorganic carbon  
160 content (TDIC) and C isotopes in Labco 12 ml Exetainer vials with no headspace. For all the  
161 water samples, the bottles were rinsed three times with filtered water from the sampled spring.  
162 Water samples for analysis of major cations and trace elements were acidified with nitric acid  
163 ( $\text{HNO}_3$  0.3N) on site. Water samples for other analyses were not acidified. All samples were  
164 stored at a temperature of 6 °C before shipment.

165 The seven gas samples were collected during the second campaign at three springs, Irénée  
166 (IRN), Manès (MANES) and Véronique (VERO), used to supply a spa and a bottled water factory.  
167 For each spring, waters are channeled through a pipe (<50 m) to a glass dome, from where the  
168 supply line goes. A small opening on top of each dome provides access to the spring gas without  
169 atmosphere contamination. The free gas was channeled through a rubber pipe to a basin filled  
170 with water from the sampled spring. Underwater, the free gas was liberated as bubbles in an  
171 upside down Exetainer vial, thus replacing the water. Gas samples were analyzed for C isotopes  
172 only.

173 For the water samples of the first campaign, alkalinity, element and isotope analyses were  
174 performed at the Bureau de Recherches Géologiques et Minières (BRGM) in Orléans. For samples  
175 of the second campaign, total dissolved inorganic carbon (TDIC), major elements, C isotopes  
176 (water and gas) and Cl isotopes were performed at the Institut de Physique du Globe de Paris  
177 (IPGP). Oxygen and H isotopes analyses were performed at the Laboratoire des Sciences du  
178 Climat et de l'Environnement (LSCE) in Saclay. Trace elements and Sr isotope analyses were  
179 performed by the Service d'Analyse des Roches et des Minéraux (SARM-CRPG) in Nancy.

180 TDIC analyses from the second campaign were made by gas chromatography and isotope  
181 ratio mass spectrometry (GC-IRMS), after releasing TDIC as  $\text{CO}_2$  by  $\text{H}_3\text{PO}_4$  acidification in the  
182 case of water samples (Assayag et al., 2006). Concentrations for each carbonate species in

183 dissolved state were computed, either using alkalinity and pH (first campaign) or TDIC and pH  
184 (second campaign), depending on which data were available. In the case of the first campaign  
185 samples, alkalinity was determined using potentiometric titration.

186 Major anions and Br concentrations were determined by ion exchange chromatography. Major  
187 cations concentrations were determined using atomic emission spectrometry (ICP). Fluoride  
188 concentrations were obtained using ion exchange chromatography for the first campaign and by  
189 direct potentiometric determination for the second campaign. Lithium concentrations were  
190 obtained by ion exchange chromatography for the first campaign and by atomic absorption  
191 spectrometry for the second campaign. Boron concentrations were obtained by inductively  
192 coupled plasma mass spectrometry (ICP-MS) for the first campaign and UV-visible spectroscopy  
193 for the second campaign. Other trace element concentrations were determined by ICP-MS for the  
194 two campaigns.

195 Carbon isotope ratios were determined together with TDIC by GC—IRMS. Oxygen and H  
196 isotope ratios were also obtained by GC-IRMS, after equilibration with a gas (H<sub>2</sub> for hydrogen and  
197 CO<sub>2</sub> for oxygen) for the first campaign. For the second campaign, Oxygen and H isotopes were  
198 obtained using the CO<sub>2</sub>-H<sub>2</sub>O equilibration method on a Finnigan Mat 252 and the WS-CRDS  
199 infrared laser method respectively. Strontium isotope ratios were determined by mass  
200 spectrometry using a triple multidynamic acquisition and a single W filament for the first  
201 campaign, and by multi-collector mass spectrometry (TIMS) for the second campaign. Precisions  
202 are comprised between 0.000006 and 0.000018. Lithium isotope analyses were performed  
203 according to techniques detailed in Millot et al., (2004). Samples were prepared in order to obtain  
204 60 ng of purified Lithium. Lithium was then separated from its matrix by ion exchange  
205 chromatography. The absence of isotopic fractionation during the purification procedure was  
206 tested by repeated analysis of the seawater standard IRMM BCR-403. The isotopic composition of  
207 Lithium was then obtained by ICP-MS using the "standard-bracketing" method and blank-  
208 corrected for the sample environment (HNO<sub>3</sub> 3%) and instrumental background noise. Chlorine  
209 isotope analyses were performed according to techniques previously detailed (Bonifacie et al.,  
210 2007; Godon et al., 2004). Because the minimum Cl concentration for high quality isotopic  
211 analyses is ~10 mg/L, we restricted our analyses to springs above this limit. Chloride from water  
212 samples were converted to CH<sub>3</sub>Cl with the following technique (Eggenkamp et al., 1994):  
213 chlorides were completely precipitated as AgCl and immediately filtrated, protected from light,  
214 and dried overnight in an oven at 80 °C, without pre-concentration. The dried filter was loaded  
215 into a pyrex tube with excess CH<sub>3</sub>I, sealed under vacuum and reacted at 80 °C for 48 hours. The  
216 tube was then cracked under vacuum and the CH<sub>3</sub>Cl product was separated from the excess CH<sub>3</sub>I  
217 by gas chromatography (2 columns filled with porapak Q). The clean CH<sub>3</sub>Cl was finally quantified

218 by a Baratron® pressure gauge, collected in sample tube and transferred to a dual inlet isotopic  
219 ratio mass spectrometer for Cl isotope analysis.

220 Non radiogenic isotope ratios are given using the  $\delta$  notation,  $\delta^{18}\text{O}_{\text{H}_2\text{O}}$  and  $\delta\text{D}_{\text{H}_2\text{O}}$  values being  
221 expressed with respect to VSMOW, and  $\delta^{13}\text{C}$ ,  $\delta^7\text{Li}$ , and  $\delta^{37}\text{Cl}$  being reported relative to PDB,  
222 LSVEC, and SMOC standards, respectively. Precisions are 0.05‰ VSMOW, 0.7‰ VSMOW, 0.1  
223 ‰ PDB, 0.5 ‰ LSVEC, and 0.05 ‰ SMOC respectively.

224 **4. Results**

225 New analyses of major and trace element concentrations, and O-, D-, Sr, Li- and Cl isotopes  
226 are presented in Table 1 and Table 2. TDIC and C isotope data are reported in Table 3. An  
227 extensive compilation of literature data for thermal springs and cold waters in La Réunion is also  
228 provided in Supplementary Material. The most important results are also summarized in Figure 1  
229 to Figure 6.

Table 1: Major elements concentrations, C, O, H, Sr, Li and Cl isotope ratios in thermal springs of Piton des Neiges analyzed in this study. (See Table B.1 for a compilation of data from previous studies)

Spring	Date	Electrical Conductivity ( $\mu\text{S}/\text{cm}$ )	pH	Temperature (°C)	Ca (mmol/L)	Mg (mmol/L)	Na (mmol/L)	K (mmol/L)	HCO <sub>3</sub> (mmol/L)	SO <sub>4</sub> (mmol/L)	Cl (mmol/L)	SiO <sub>2</sub> (mmol/L)	CO <sub>3</sub> (mmol/L)	NH <sub>4</sub> (mmol/L)	NO <sub>2</sub> (mmol/L)	NO <sub>3</sub> (mmol/L)	$\delta^{18}\text{O}$ VSMOW (%)	$\delta\text{D}$ VSMOW (%)	$^{87}\text{Sr}/^{86}\text{Sr}$	$\delta^7\text{Li}$ LSVEC (%)	$\delta^{37}\text{Cl}$ SMOC (%)
AGS	17/06/2015	1746	6.5	21.1	6.8	3.5	1.7	0.1	14.5	4.1	0.0	1.3	b.d.l.	b.d.l.	b.d.l.	-6.70	-41.6	0.704317	9.1		
BACH	15/06/2015	1260	6.9	25.6	2.9	2.6	3.9	0.1	14.4	0.1	0.1	1.3	b.d.l.	b.d.l.	b.d.l.	-6.7	-37.2	0.704300	11.9		
BACH*	Sanjuan et al., 2001	1540	7.4	19.4	3.6	3.5	5.5	0.2	18.7	0.2	0.1	1.5	b.d.l.	b.d.l.	b.d.l.	-6.7	-37.2	0.704300	13 <sup>1</sup>		
BB	05/05/2017	1699	6.7	25.1	4.1	3.3	5.9	0.1	18.1	2.3	0.4	2.0	b.d.l.	b.d.l.	b.d.l.	0.01	-8.06	-53.1	0.704139	0.3	
BB	Sanjuan et al., 2001	1610	6.7	22.6	4.2	3.4	5.5	0.1	15.4	2.1	0.3	1.9	b.d.l.	b.d.l.	b.d.l.	-8.2	-54.3	0.704142	18 <sup>1</sup>		
BR12	Sanjuan et al., 2001	1430	6.3	36.3	1.6	1.3	10.8	0.3	11.6	2.1	0.6	2.1	b.d.l.	b.d.l.	b.d.l.	-8.2	-50.5	0.704162	2 <sup>1</sup>		
BR14	08/09/2017	1764	6.8	37.2	1.5	2.5	12.4	0.3	24.7	0.9	1.2	2.5	b.d.l.	b.d.l.	b.d.l.	-8.53	-53.7	0.704179		-0.4	
BR16	29/10/2017	3370	6.5	29.1	0.2	3.1	25.0	1.0	22.7	0.5	5.1	2.6	b.d.l.	b.d.l.	b.d.l.	0.00	-8.67	-53.3	0.704162	0.0	
BR16	30/07/2016	2530	6.8	25.9	0.4	2.4	18.4	0.9	21.7	0.4	3.2	2.0	0.01	b.d.l.	b.d.l.	-8.41	-52.0	0.704165	0.1		
BR21	23/08/2016	1256	6.2	25.1	1.8	0.6	9.8	0.1	7.4	0.5	0.4	0.6	0.00	b.d.l.	b.d.l.	-8.07	-51.7	0.704249		0.4	
DUP	15/06/2015	714	8.1	23.3	1.4	1.3	2.8	0.1	7.2	0.4	0.1	1.0	b.d.l.	b.d.l.	b.d.l.	-6.50	-38.4	0.704224	13.3		
EDN	16/05/2015	1855	6.4	25.5	3.2	6.2	4.0	0.2	23.0	0.1	0.0	2.3	b.d.l.	b.d.l.	b.d.l.	-6.50	-38.7	0.704237	9.6		
GDS	17/06/2015	1234	7.7	18.7	4.7	2.2	1.3	0.1	8.8	3.3	0.0	0.8	b.d.l.	b.d.l.	b.d.l.	-5.90	-33.1	0.704330	14.5		
GDS	Sanjuan et al., 2001	6.6	18.6	4.6	2.2	1.3	0.1	8.4	2.9	0.1	0.7	b.d.l.	b.d.l.	b.d.l.	-4.9	-23.5	0.704336	16.6 <sup>1</sup>			
IRN	05/05/2017	2510	6.5	35.1	0.4	4.2	15.0	0.2	0.0	1.0	0.2	2.3	b.d.l.	b.d.l.	b.d.l.	0.00	-8.05	-51.0			
IRN	15/06/2017	2500	6.4	36	0.1	4.1	14.8	0.2	24.6	1.0	0.2	2.4	b.d.l.	b.d.l.	b.d.l.	0.00	-8.10	-51.2	0.704168		
IRN	28/07/2017	2520	6.4	35.6									b.d.l.	b.d.l.	b.d.l.	-8.09	-51.2				
IRN	30/08/2017	2560	6.4	36.2	0.1	4.2	15.5	0.2	29.0	1.0	0.2	2.4	b.d.l.	b.d.l.	b.d.l.	0.00	-8.04	-50.9			
IRN	25/09/2017	2560	6.6	36.2	0.1	4.1	15.1	0.2	20.0	1.0	0.2	2.4	b.d.l.	b.d.l.	b.d.l.	0.00	-7.89	-50.9			
IRN	26/10/2017	2570	6.4	34.3	0.1	4.3	15.3	0.2	25.3	1.0	0.2	2.4	b.d.l.	b.d.l.	b.d.l.	0.00	-8.06	-51.0			
IRN	29/11/2017	2570	6.7		0.1	4.2	15.1	0.2	20.5	1.0	0.2	2.5	b.d.l.	b.d.l.	b.d.l.	0.00	-8.14	-51.1	0.704181		
IRN	Sanjuan et al., 2001	2370	6.0	37.8	4.6	4.6	16.1	0.2	31.2	1.1	0.1	2.6	b.d.l.	b.d.l.	b.d.l.	-8.2	-51.3	0.704169	12 <sup>1</sup>		
MAN	16/06/2015	1395	6.6	30.6	3.3	2.7	4.4	0.2	16.6	0.1	0.1	1.8	b.d.l.	b.d.l.	b.d.l.	-7.20	-43.4	0.704273	10.0		
MAN	Sanjuan et al., 2001	1580	6.6	30.6	4.1	3.4	5.0	0.2	19.2	0.1	0.1	2.0	b.d.l.	b.d.l.	b.d.l.	-7.6	-43.9	0.704282	8 <sup>1</sup>		
MAN G	Sanjuan et al., 2001	1333	7.9	19	4.0	3.0	2.7	0.1	15.8	0.1	0.0	1.6	b.d.l.	b.d.l.	b.d.l.	-7.0	-39.8		7.5 <sup>1</sup>		
MANES	15/06/2017	2310	6.4	29.8	0.3	3.9	13.0	0.2	22.1	0.9	0.2		b.d.l.	b.d.l.	b.d.l.	0.00	-8.04	-51.5			
MANES	Sanjuan et al., 2001	2260	5.3	31	4.0	4.1	12.9	0.2	26.7	0.8	0.1	2.1	b.d.l.	b.d.l.	b.d.l.	-8.2	-54.3		15.7 <sup>1</sup>		
OLIV1	Sanjuan et al., 2001	994	7.3	18.9	1.4	1.3	5.7	0.1	8.2	0.5	1.4	0.7	b.d.l.	b.d.l.	b.d.l.	-4.5	-6.5	-40.1		11.6 <sup>1</sup>	
OLIV2	Sanjuan et al., 2001	4980	6.1	26	4.1	4.6	47.0	0.5	42.7	3.2	12.9	0.8	b.d.l.	b.d.l.	b.d.l.	1.8	-7.8	-45.9	0.704270	34.8 <sup>1</sup>	
PISSA	Sanjuan et al., 2001	1190	6.7	18.4	4.4	1.4	3.1	0.0	11.6	1.3	0.0	1.3	b.d.l.	b.d.l.	b.d.l.	-6.7	-41.4		11.1 <sup>1</sup>		
RB1	15/10/2016	929	6.0	19.8	1.0	1.8	1.2	0.2	7.9	0.1	0.1	1.6	0.00	b.d.l.	b.d.l.	-6.50	-37.1	0.704308			
RFOUQ	Sanjuan et al., 2001	1000	7.4	19.2	2.9	2.3	2.2	0.0	11.3	0.3	0.0	0.7	b.d.l.	b.d.l.	b.d.l.	-6.5	-37.9		21.8 <sup>1</sup>		
RR1	30/07/2016	1586	6.2	32.5	0.6	1.4	10.3	0.3	7.4	0.9	1.5	1.8	0.00	b.d.l.	b.d.l.	-8.48	-56.3	0.704167		0.2	
sRMAT	Sanjuan et al., 2001		7.9	18	1.9	6.0	3.7	0.3	17.7	0.5	0.1	1.2	b.d.l.	b.d.l.	b.d.l.	-5.9	-36.5		12 <sup>1</sup>		
sRMAT2	Sanjuan et al., 2001		716	7.1	21.2	1.9	1.4	1.9	0.1	8.2	0.1	0.1	0.5	b.d.l.	b.d.l.	b.d.l.	-6.2	-35.5		13 <sup>1</sup>	
sRMAT3	Sanjuan et al., 2001		716	7.1	21.2	1.9	1.4	1.9	0.1	8.2	0.1	0.1	0.5	b.d.l.	b.d.l.	b.d.l.	0.11			20.6 <sup>1</sup>	
TB	22/11/2017	1410	6.3	34.4	1.2	1.0	9.4	0.3	12.0	0.6	0.7	1.1	b.d.l.	b.d.l.	b.d.l.	-6.42	-38.7	0.704194		0.3	

Spring	Date	Electrical Conductivity ( $\mu\text{S}/\text{cm}$ )	pH	Temperature ( $^{\circ}\text{C}$ )	Ca (mmol/L)	Mg (mmol/L)	Na (mmol/L)	K (mmol/L)	$\text{HCO}_3$ (mmol/L)	$\text{SO}_4$ (mmol/L)	Cl (mmol/L)	$\text{SiO}_2$ (mmol/L)	$\text{CO}_3$ (mmol/L)	$\text{NH}_4$ (mmol/L)	$\text{NO}_2$ (mmol/L)	$\text{NO}_3$ (mmol/L)	$\delta^{18}\text{O}$ vSMOW (‰)	$\delta D$ vSMOW (‰)	$^{87}\text{Sr}/^{86}\text{Sr}$	$\delta^{7\text{Li}}$ LSVEC (‰)	$\delta^{37}\text{Cl}$ SMOC (‰)
TBA	15/06/2015	1718	6.3	26.6	4.0	2.5	7.1	0.2	17.0	1.0	0.1	2.1	b.d.l.	b.d.l.	b.d.l.	0.00	-6.69	-41.1	0.704333	11.5	
TR	21/07/2017	379	7.3	20.8	0.8	0.8	0.7	0.0	3.1	1.1	0.1	0.5				0.00			0.704308		
TR	30/01/2018	1016	7.5	20.8	2.4	2.7	1.1	0.1	4.2	5.1	0.1	0.6				0.00					
VERO	15/06/2017	1938	6.2	29.5	0.2	3.3	10.6	0.2	20.8	0.7	0.1					0.00	-7.96	-51.6			
VERO	30/08/2017	1986	6.2	29.7	0.2	3.4	10.7	0.2	16.2	0.7	0.1					0.00	-7.96	-51.2			
VERO	Sanjuan et al., 2001	2010	5.4	30.3	3.6	3.7	10.9	0.1	23.5	0.7	0.1	2.0	b.d.l.	b.d.l.	b.d.l.	-8.1	-51.2			14.1 <sup>1</sup>	

<sup>1</sup>  $\delta^{37}\text{Cl}$  and  $\delta^7\text{Li}$  data on samples from Sanjuan et al (2001) are from this study

233

Table 2: Trace elements concentrations in thermal springs of Piton des Neiges analyzed in this study. (See Table B.2 for a compilation of data from previous studies)

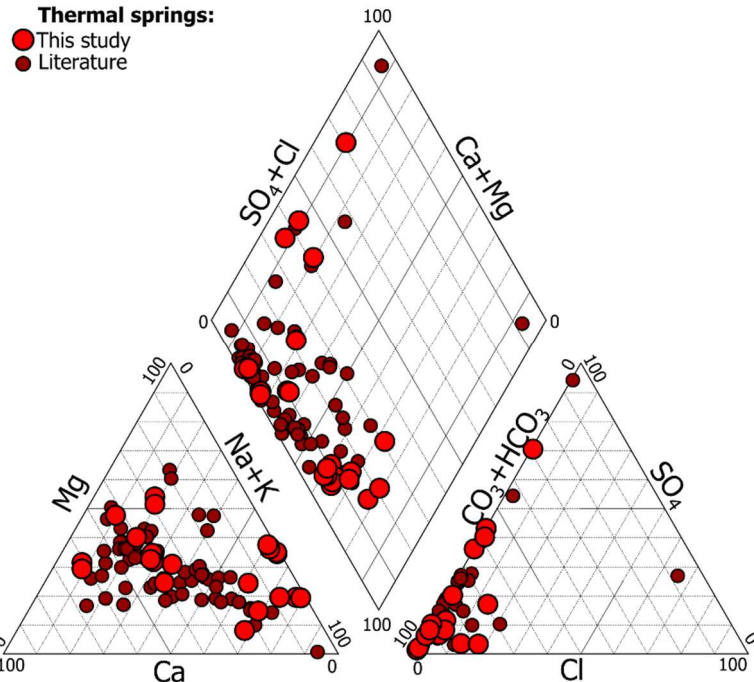
<sup>1</sup> Li concentrations on samples from Sanjuan et al (2001) are from this study

236 Table 3: Carbon species distribution and isotopic ratios in waters and gas in thermal springs of Piton des Neiges.  
 237 (See Table B.3 for a compilation of data from previous studies).

Spring	pH	Temperature (°C)	TDIC (mM)	H <sub>2</sub> CO <sub>3</sub> (mM)	HCO <sub>3</sub> (mM)	$\delta^{13}\text{C}_{\text{TDIC}} (\text{\textperthousand})$ PDB	$\delta^{13}\text{C}_{\text{CO}_2} (\text{\textperthousand})$ PDB
BACH	6.85	25.6	18.92	4.55	14.38	1.40	
BB	6.7	25.1	26.2	8.10	18.10	-1.39	
BR14	6.8	37.2	32.61	7.86	24.74	-0.78	
BR16	6.5	29.1	38.13	15.39	22.73	0.6	
BR21	6.2	25.1	17.93	10.50	7.43	2.98	
DUP	8.1	23.3	7.36	0.13	7.23	3.40	
EDN	6.41	25.5	43.03	20.03	23.00	3.00	
GDS	7.7	18.7	9.18	0.39	8.79	1.70	
IRN	6.5	35.1	40.35	15.79	24.56	-1.22	
IRN	6.7	35	40.73	11.76	28.97	-0.86	-5.26
IRN	6.4	36.2	38.03	21.73	16.29	-0.78	
IRN	6.4	36	36.16	16.12	20.04	-0.51	-5.39
IRN	6.6	36.2	38.18	12.84	25.33	-0.5	-5.39
IRN	6.4	34.3	37.22	16.70	20.52	-0.36	-5.35
MAN	6.56	30.6	26.84	10.27	16.57	1.60	
MANES	6.4	30.5	40.65	18.56	22.08	-1.43	-5.63
RB1	5.95	19.8	29.30	21.41	7.89	-1.91	
RR1	6.17	32.5	17.77	10.37	7.40	2.61	
TB	6.3	34.4	24.31	12.30	12.01	-1.72	
TR	7.3	20.8	3.53	0.38	3.15	-8.02	
TR	7.5	20.8	4.5	0.31	4.18	-6.36	
VERO	6.2	29.7	37.83	21.68	16.15	-2.16	-5.99
VERO	6.4	29.3	38.48	17.69	20.79	-2.08	-5.79

238  
 239 Temperature, pH and electrical conductivity values at the spring outlets are in the range of  
 240 19.2 – 48.0 °C, 5.3 – 7.6, and 312 – 3370 µS/cm, respectively (Table 1). Thermal waters show a  
 241 mixed composition between Na-Ca-Mg (Figure 2). Most springs are bicarbonate dominated. A few  
 242 springs, however, show a trend toward the sulfate and/or chloride pole. For instance, the Tuf  
 243 Rouge spring (TR), is sulfate dominated with sulfate concentrations reaching 765 ppm. The  
 244 spring of Mafate (MF1) is the only chloride dominated spring. For the majority of springs, the  
 245 relative proportions of major elements display little variation over time (1 s.d. of Na+K, Ca+Mg,  
 246 SO<sub>4</sub>+Cl, HCO<sub>3</sub> mole fractions ≤ 8%), with the exception of TR that shows larger temporal  
 247 fluctuations (≤ 18%).

248



249

250      Figure 2: Piper diagram for thermal springs of Piton des Neiges. Literature data are from Belle (2014), Frissant  
 251      et al. (2003), Iundt et al. (1992), Lopoukhine and Steltjes (1978), Louvat and Allègre (1997), and Sanjuan et al.  
 252      (2001). Most springs are bicarbonate dominated.

253

254      Total alkalinity ( $\text{HCO}_3^-$ ) varies from 56 to 2769 ppm. Expressed as TDIC concentrations,  
 255      springs also analyzed for  $\delta^{13}\text{C}$  cluster between of 3.5 and 99.2 mM, with two outliers, the MANES  
 256      spring at 127.8 mmol/L and the OLIV2 spring at 283.7 mmol/L (Table 3).  $\delta^{13}\text{C}_{\text{TDIC}}$  data range  
 257      from -8.0 to 3.2 ‰, values for the TR spring (-8.0 and -6.4 ‰) being significantly lower than  
 258      those of other springs.  $\delta^{13}\text{C}_{\text{CO}_2}$  values of spring gas range from -6.7 to -5.3 ‰.

259       $\delta^{18}\text{O}_{\text{H}_2\text{O}}$  and  $\delta\text{D}_{\text{H}_2\text{O}}$  values for thermal springs range from -8.67 to -4.9 ‰ and from -56.3 to -  
 260      23.5 ‰ VSMOW, respectively, without any shift from the Local Meteoric Water Line (Table 1,  
 261      Table B.1, Figure 3). Our new O and D isotopic analyses fall within  $\pm 0.1$  ‰ of previous values  
 262      for the same springs (e.g. IRN, VERO). Importantly, thermal springs are among the most  
 263      depleted waters in  $^{18}\text{O}$  and D of Réunion, their  $\delta^{18}\text{O}_{\text{H}_2\text{O}}$  and  $\delta\text{D}_{\text{H}_2\text{O}}$  values being more negative  
 264      than those of rivers and groundwater ( $-7.1 \leq \delta^{18}\text{O}_{\text{H}_2\text{O}} \leq -3.0$  ‰ and  $-45.0 \leq \delta\text{D}_{\text{H}_2\text{O}} \leq -11.4$  ‰),  
 265      and only comparable to those of water samples associated with cyclonic events ( $-11.8 \leq \delta^{18}\text{O}_{\text{H}_2\text{O}} \leq -7.53$  ‰ and  $-78.0 \leq \delta\text{D}_{\text{H}_2\text{O}} \leq -46.1$  ‰) or to the most depleted rainwater collected at high  
 266      altitude ( $\geq 2000$  m,  $\delta^{18}\text{O}_{\text{H}_2\text{O}} = -7.6$  ‰ and  $\delta\text{D}_{\text{H}_2\text{O}} = -47.0$  ‰, Table C.1).

268      Major and trace element concentrations are reported in Figure 5 as a function of chloride. In  
 269      comparison with cold waters, thermal springs are systematically enriched in Na, K, Mg, B, Li and  
 270       $\text{SO}_4$  for a given Cl concentration (Table 1 and Table 2, Figure 5). Li concentrations of rivers RFER,  
 271      RBACH and RMAT are respectively 0.01, 0.29 and 0.29  $\mu\text{mol/L}$ .

272 The  $^{87}\text{Sr}/^{86}\text{Sr}$  ratios of Piton des Neiges thermal springs, reported in Table 1 and Figure 5, fall  
273 in a much narrower range (0.704142 to 0.704336) than those of La Réunion cold waters  
274 (0.704141 to 0.708227). This narrow range is similar to that of Piton des Neiges rocks (0.704041  
275 to 0.704368), and is much lower than that of seawater offshore Réunion Island (0.709179).

276  $\delta^7\text{Li}$  values of most thermal springs range between +7.5 ‰ and +21.8 ‰ (Table 1 and  
277 Figure 6), well below seawater (+31 ‰). There are, however, two extreme  $\delta^7\text{Li}$  values in the  
278 thermal spring dataset, one at +2 ‰ (BR12) and one at +34.8 ‰ (OLIV2).  $\delta^7\text{Li}$  values of rivers  
279 RFER, RBACH and RMAT are respectively of 25.2, 12.1, and 9.7 ‰. The  $\delta^{37}\text{Cl}$  of thermal springs  
280 ranges from the value of seawater (0 ‰) and +0.40 ‰, except for one spring (BR14) showing  
281 a negative value of -0.35 ‰ (Table 1 and Figure 6).

282 **5. Discussion**

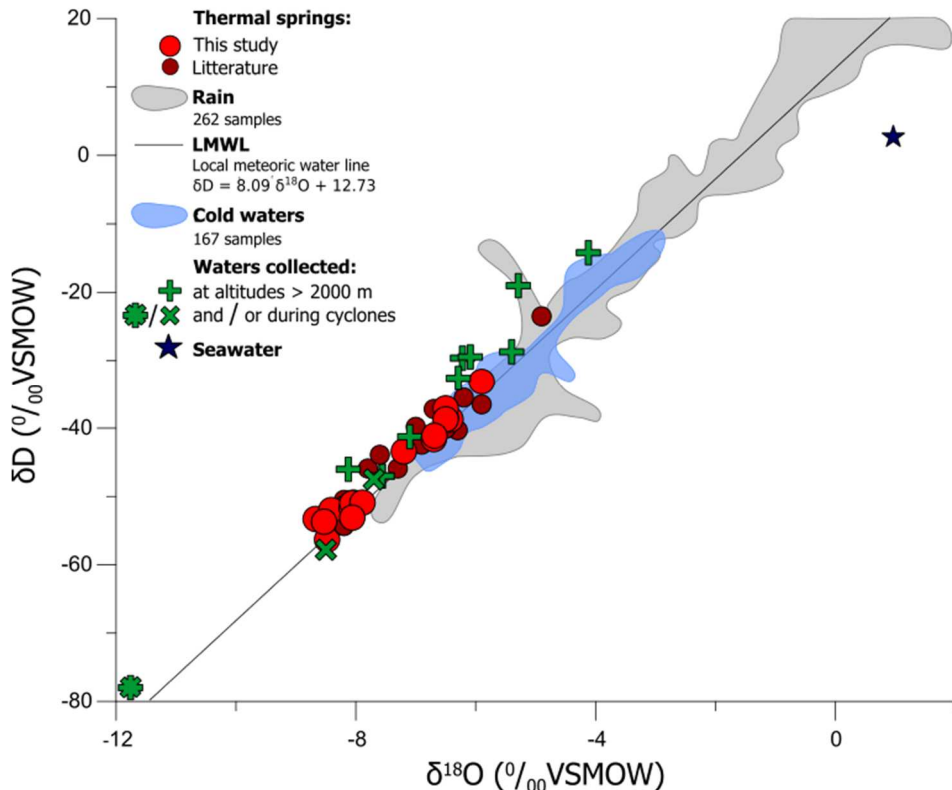
283 **5.1. Origin of water**

284 Major-trace element compositions and isotope analyses are powerful tools to identify the  
285 reservoirs supplying the different species in solution, and thus the origin and pathways of  
286 hydrothermal fluids in the massif of Piton des Neiges volcano. This identification work must begin  
287 with water reservoirs. In a  $\delta^{18}\text{O}_{\text{H}_2\text{O}}$  vs  $\delta\text{D}_{\text{H}_2\text{O}}$  diagram, the plot of Piton des Neiges thermal springs  
288 on the local meteoric water line (LMWL) indicates that water is of meteoric origin (Figure 3). As  
289 no data significantly depart from the LMWL, it can be inferred that processes such as seawater  
290 contamination, evaporation, or exchange with  $\text{CO}_2$ ,  $\text{H}_2\text{S}$  or minerals do not influence largely the O  
291 and H isotope composition of thermal springs.

292 In addition, the strong  $^{18}\text{O}$  and D depletion observed in thermal springs compared to other  
293 waters may be used to constrain their origin more precisely. Thermal springs have very low  
294  $\delta^{18}\text{O}_{\text{H}_2\text{O}}$  and  $\delta\text{D}_{\text{H}_2\text{O}}$  values compared to rivers, groundwater or to the majority of rainfalls from La  
295 Réunion available in the literature (Grunberger, 1989; Nicolini et al., 1991; Aunay and Gourcy,  
296 2007; Aunay et al., 2012; Rogers et al., 2012; Aunay et al., 2013; Petit et al., 2013a, 2013b;  
297 Belle, 2014; Gourcy et al., 2018), suggesting a contribution of depleted waters like high altitude  
298 rainfalls and cyclones. Indeed, the isotopic signature of rainfalls being strongly controlled by the  
299 amount of condensed water (distillation effect), they are usually increasingly depleted in heavy  
300 isotopes with increasing altitude as the air masses cool and condensate (Hoefs, 2015). In the  
301 existing database for Réunion Island, the highest altitude rainfalls sampled so far outside of a  
302 cyclonic event ( $\delta^{18}\text{O}_{\text{H}_2\text{O}} = -7.1$  ‰,  $\delta\text{D}_{\text{H}_2\text{O}} = -41.26$  ‰ at 2250 m for the rainy season of 1985-  
303 1986) do not reach the depletion of thermal springs (up to -8.67 ‰ and -56.3 ‰ for  $\delta^{18}\text{O}_{\text{H}_2\text{O}}$   
304 and  $\delta\text{D}_{\text{H}_2\text{O}}$ , respectively), and the estimated altitude gradients are not strong enough to explain

305 their negative  $\delta^{18}\text{O}_{\text{H}_2\text{O}}$  vs  $\delta\text{D}_{\text{H}_2\text{O}}$  signature (Grunberger, 1989; Nicolini et al., 1998, 1991).  
306 Nevertheless, it cannot be excluded that high altitude rainfalls yet to be analyzed (for instance  
307 close to the Piton des Neiges summit at 3070 m) may control the signature of spring waters.  
308 Alternatively, cyclones are another candidate, because those extreme rainfalls represent the most  
309 isotopically depleted reservoir of meteoric waters (Lawrence and Gedzelman, 1996). The lowest  
310  $\delta^{18}\text{O}_{\text{H}_2\text{O}}$ ,  $\delta\text{D}_{\text{H}_2\text{O}}$  values of thermal springs are in the range of those from cyclone waters (Aunay  
311 and Gourcy, 2007; Nicolini et al., 1989). In consequence, we interpret thermal spring waters as  
312 being supplied largely by cyclones, with a possible contribution from high altitude ( $\geq 2000$  m)  
313 rainfalls. From the comparison of our new analyses with available literature data, it seems that  
314 the O, H isotope composition of springs is very steady over several decades (e.g. for the IRN  
315 spring, Table 1 and supplementary material), and is barely influenced by seasonal variations of  
316 rainfall supply. However, the database for rain isotope ratios in La Réunion does not allow us to  
317 explore the inter-annual and inter-cyclone variability of isotopes ratios that could fall in the range  
318 of the thermal waters (Guilpart et al., 2017). Whatever their origin, this  $^{18}\text{O}$  and D depletion  
319 indicates that thermal waters do not completely homogenize with cold groundwater, which  
320 implies that their pathway is disconnected from the superficial water table.

321 The absence of  $^{18}\text{O}$  enrichment of thermal waters relative to the LMWL also indicates that the  
322 isotopic exchange between rocks and water is very limited. As this is well-known, the oxygen  
323 isotopic exchange kinetics between water and rocks (mainly silicate and carbonate minerals) is  
324 very slow at atmospheric temperature and becomes significant only at high temperature (Panichi  
325 and Gonfiantini, 1977). For this reason,  $^{18}\text{O}$  enrichment relative to local groundwater is observed  
326 for most of the worldwide geothermal waters discharged from high-temperature wells  $> 180$  °C  
327 (Panichi and Gonfiantini, 1981). The water/rock ratio may also be an influent parameter on the  
328  $^{18}\text{O}$  enrichment of the waters. For example, at similar high temperatures of 300-350 °C, the  $\delta^{18}\text{O}$   
329 values for the Los Humeros geothermal waters (Mexico, Tello et al., 2000), indicate a much more  
330 significant  $^{18}\text{O}$  enrichment from the water-rock interactions than that for the Krafla geothermal  
331 waters (Iceland, Sveinbjornsdottir et al., 1986), for which the water-rock ratio is higher. In  
332 comparison with these geothermal systems, the lack of oxygen isotopic exchange between rocks  
333 and thermal waters at Piton des Neiges suggests that their temperatures of interaction are  
334 relatively low ( $< 180$  °C) and/or that the water/rock ratios are high enough to buffer the isotopic  
335 signature of Réunion basalts (5.5 – 6.6 ‰).



336

337     Figure 3: Comparison of  $\delta^{18}\text{O}_{\text{H}_2\text{O}}$  vs  $\delta\text{D}_{\text{H}_2\text{O}}$  values for Piton des Neiges hot springs with rainfalls, cold waters  
 338     (rivers and groundwater), and seawater from La Réunion. Datasets for rainwater and cold waters (grey and blue  
 339     shaded contours, respectively) do not include waters collected at altitudes > 2000 m and waters associated with  
 340     cyclonic events. These two subsets, detailed in Table C.1, are represented separately: cyclone waters (tilted  
 341     green crosses), waters collected at altitudes > 2000 m (straight green crosses), cyclone waters collected at  
 342     altitudes > 2000 m (combined tilted and straight green crosses). The local meteoric water line is the linear  
 343     regression for the total rainwater dataset. Thermal springs plot on the meteoric water line. Some thermal springs  
 344     show a strong depletion in  $^{18}\text{O}$  and D compared to low-altitude rainfalls and cold waters. Literature data are  
 345     from Grunberger (1989), Nicolini et al. (1991), Sanjuan et al. (2001), Frissant et al. (2005), Aunay and Gourcy  
 346     (2007), Aunay et al. (2012), Rogers et al. (2012), Aunay et al. (2013), Petit et al. (2013a; 2013b), Belle (2014),  
 347     and Gourcy et al. (2018).

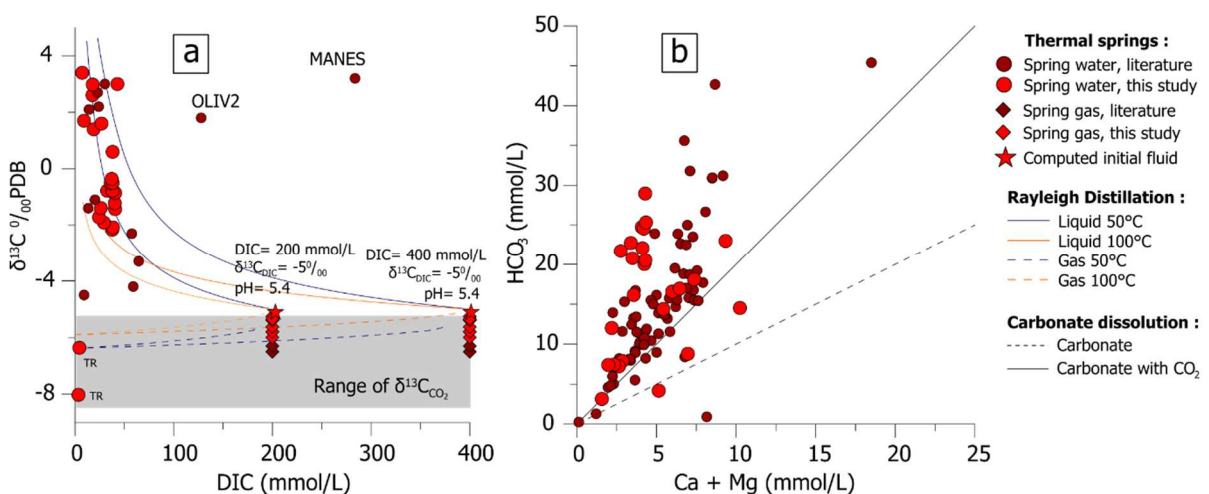
348     5.2. Origin of carbon

349     Because  $\text{CO}_2$  bubbling is observed at the outlet of several springs (e.g. IRN, BC), the original  
 350     composition of thermal waters prior to degassing must be reconstructed for interpreting TDIC  
 351     and  $\delta^{13}\text{C}$  data. Following the equations detailed in Ruzié et al. (2013), we thus estimated the  
 352     initial (pre-degassing) TDIC and  $\delta^{13}\text{C}_{\text{TDIC}}$  as a function of the final TDIC,  $\delta^{13}\text{C}_{\text{TDIC}}$ ,  $\delta^{13}\text{C}_{\text{CO}_2}$ ,  
 353     temperature, and pH using an open system Rayleigh distillation law. As  $\text{CO}_2$  degassing  
 354     fractionates  $^{12}\text{C}$  into the gas phase and  $^{13}\text{C}$  into the liquid phase, the initial  $\delta^{13}\text{C}_{\text{TDIC}}$  of the solution  
 355     is bracketed between the final values of  $\delta^{13}\text{C}_{\text{TDIC}}$  (-4.5 to 3.4 ‰) and  $\delta^{13}\text{C}_{\text{CO}_2}$  (-6 to -5.3 ‰). For  
 356     the majority of thermal springs, the initial fluid that best fits the observed compositions and  
 357     carbon isotopic signatures has thus a  $\delta^{13}\text{C}_{\text{TDIC}}$  of -5 ‰, a pH of 5.4, and a TDIC of 200 to 400  
 358     mmol/L (Figure 4a). This initial fluid is inferred to degas at a temperature of 50 to 100 °C, and a  
 359      $\text{P}_{\text{CO}_2}$  of 0.9 to 3 MPa. Our pre-degassing  $\delta^{13}\text{C}_{\text{TDIC}}$  value of -5 ‰ is consistent with a mantle

360 carbon signature (Deines, 2002). It is also in agreement with the  $\delta^{13}\text{C}_{\text{CO}_2}$  of fumaroles (-4.1 ‰, 361 Marty et al., 1993) and the  $\delta^{13}\text{C}$  of xenolith fluid inclusions (-4.6 to -3.7 ‰ (Trull et al., 1993), at 362 Piton de la Fournaise.

363 Two  $\delta^{13}\text{C}_{\text{TDIC}}$  data belonging to the TR spring (-8 and -6.4 ‰) are too low to come from the 364 Rayleigh distillation of a solution at -5 ‰. These low values are possibly explained by a biogenic 365 end-member contribution ( $\delta^{13}\text{C}_{\text{CO}_2} \leq -20$  ‰) or by re-dissolution of degassed and fractionated 366 magmatic  $\text{CO}_2$  (Liuzzo et al., 2015). Alternatively, it is possible that magmatic degassing 367 processes might also fractionate exsolved carbon (Boudoire et al., 2018). Two other springs, 368 MANES and OLIV2, have too high TDIC values to explain their  $\delta^{13}\text{C}_{\text{TDIC}}$  by Rayleigh distillation 369 from the above initial solution. These abnormal values may either correspond to an extremely 370 high initial TDIC ( $\geq 1$  mol/L), or to an incorrect measurement of the pH at the outlet. The second 371 interpretation is favored in the case of MANES, showing a surprisingly low pH value for this 372 analysis (5.33) compared to anterior and posterior pH measurements (6 to 6.6) of the same 373 spring. For all the other springs, we conclude that the origin of dissolved carbon is essentially 374 magmatic, a conclusion also reached by Marty et al. (1993).

375 Studies of secondary minerals at Piton des Neiges report the occurrence of abundant 376 hydrothermal calcite precipitation in the porosity of basalts (Famin et al., 2016; Rançon, 1985), 377 deposited by past episodes of magmatic carbon degassing. Such calcite may represent a 378 significant carbon pool with a magmatic  $\delta^{13}\text{C}$  signature. This raises the question as to whether 379 the dissolved magmatic carbon found in springs is supplied by a re-dissolution of secondary 380 calcite, or by an actively degassing magma. In a  $\text{HCO}_3$  vs  $(\text{Ca} + \text{Mg})$  diagram, the majority of 381 springs plot above the carbonate dissolution line, even in presence of extra  $\text{CO}_2$  (Figure 4b). 382 Calcite dissolution alone is thus unable to explain the  $\text{HCO}_3$  enrichment. This leaves primary 383 degassing of an active magma as the largest source of TDIC.



385 Figure 4: (a)  $\delta^{13}\text{C}_{\text{TDIC}}$  (‰ PDB) versus Dissolved Inorganic Carbon (mM) for water and gas in thermal springs of 386 Piton des Neiges, La Réunion. Degassing lines are represented for two possible initial fluid concentrations and for

387 different temperatures. Error bars are shorter than symbols. (b)  $\text{HCO}_3^-$  versus  $\text{Ca} + \text{Mg}$  molar concentrations for  
388 thermal springs of Piton des Neiges, with equilibrium lines for carbonate (calcite) dissolution with and without  
389 carbon dioxide. Thermal springs are enriched in  $\text{HCO}_3^-$  compared to calcite dissolution lines. Literature data are  
390 from (Aunay et al., 2013; Frissant et al., 2003; Iundt et al., 1992; Lopoukhine and Steltjes, 1978; Louvat and  
391 Allègre, 1997; Marty et al., 1993; Sanjuan et al., 2001).

392        5.3. Origin of mineralization

393        *Major and trace elements*

394        The absence of  $\text{NO}_3^-$  in springs, and their location at altitudes usually higher than inhabited or  
395 farmed lands, indicate that there is no significant anthropogenic contribution to this  
396 mineralization. Given the magmatic origin of carbon, other species dissolved in hydrothermal  
397 waters may be supplied by degassing magmas. Additionally or alternatively, dissolved species  
398 may come from seawater mixing or water-rock interaction such as rock leaching or dissolution of  
399 fossil fumarolic deposits. Seawater mixing and water-rock interaction may be explored using  
400 diagrams of species concentration vs [Cl] (Figure 5). In such diagrams, dissolved species  
401 concentrations barely show any correlation with [Cl] below a threshold of  $\sim 0.2$  mmol/L Cl, and  
402 plot on the line of basalt compositions. This suggests that for springs having low Cl  
403 concentrations (hereafter labelled “Group 1”), leaching of basaltic rocks is the main source of  
404 mineralization (Figure 5a-b). Spring outlets provide a lower bound of  $\sim 50$  °C for the temperature  
405 of water-rock interaction. Above 0.2 mmol/L Cl (Group 2), most species depart from a simple  
406 rock leaching line. For instance, some springs display Na/Cl or K/Cl ratios compatible with a small  
407 contamination ( $\leq 3$  mol%) of rock-leaching waters by seawater (Group 2a, Figure 5 c-g).  
408 However, other springs have too elevated F, B, Li, Cs, and Rb concentrations at a given [Cl] to be  
409 explained by mixing of rock-leaching waters with seawater. The high F/Cl, B/Cl, Li/Cl, Cs/Cl, and  
410 Rb/Cl ratios in these springs (Group 2b) require an additional source for these elements, such as  
411 selective mineral dissolution or magmatic degassing. We note that Cl, F, B, Li, Cs and Rb are  
412 volatile elements in magmas from Piton de la Fournaise undergoing low-pressure differentiation  
413 and degassing (Vlastélic et al., 2011). This analogy pleads in favor of a dissolution of gas or  
414 fumarolic deposits from a differentiated melt within Piton des Neiges. Given the lack of  
415 correlation between TDIC and Cl, F, B, Li, Cs or Rb concentrations, the source of these species is  
416 independent from the carbon source.

417 Table 4: Classification of thermal springs of Piton des Neiges in three groups according to mineralization  
 418 processes, and their associated geochemical profiles in major trace elements,  $\delta^7\text{Li}$  and  $\delta^{37}\text{Cl}$  values.

	<b>Group 1</b>	<b>Group 2a</b>	<b>Group 2b</b>
Thermal springs	AGS, BACH, BC, BE, BR1, BR10, BR11, BR12, BR13, BR15, BR18, BR2, BR27, BR3, BR4, BR5, BR6, BR7, BR8, BR9, DUP, EDN, FJ1, FJ2, FJ3, G1, G2, G3, G4, GDS, IRN, MAN, MAN G, MANES, OLIVbis, PC, PISSA, RB1, RFOUQ, sRMAT, sRMAT2, TBA, TR, VERO	BB, MF1, OLIV2, sRMAT3	BR12, BR14, BR16, BR17, BR21, IMA, OLIV1, RR1, TB
$\delta^{18}\text{O}$ and $\delta\text{D}$	-8.67 to -4.9 ‰ VSMOW and 56.3 to -23.5 ‰ VSMOW Meteoric water, mostly cyclone and/or high altitude rains		
$\delta^{13}\text{C}$	-8.0 to 3.2 ‰ PDB Mostly magmatic $\text{CO}_2$		
Major and trace elements	$\text{Cl} < 0.2 \text{ mmol/L}$ and enrichment in other elements along basalt composition	$\text{Cl} > 0.2 \text{ mmol/L}$ and enrichment in other elements by seawater mixing	$\text{Cl} > 0.2 \text{ mmol/L}$ and enrichment in Na, F, B, Li, Cs, Rb above seawater mixing
$^{87}\text{Sr}/^{86}\text{Sr}$	0.704142 to 0.704336 Interaction with Reunion Island rocks		
$\delta^7\text{Li}$	+7.5 to +16.6 ‰ LSVEC Interaction with basalt	+18 to +34.8 ‰ LSVEC Mixing with seawater	+2 ‰ LSVEC Interaction with differentiated magma or their gas products/condensates
$\delta^{37}\text{Cl}$	No data	+0.06 to +0.35 ‰ SMOC Mixing with seawater	-0.35 to +0.4 ‰ SMOC Mixing with seawater and magmatic input
$\delta^{34}\text{S}$	+2.0 to +5.8 ‰ CDT Magmatic sulfur	+3.0 to +8.9 ‰ CDT Magmatic sulfur with seawater mixing	+4.8 ‰ CDT Mostly magmatic sulfur
Spatial repartition	In Sill zones, rift zone N30°E and inside the proposed caldera rim	Outside the proposed caldera rim	Near syenite intrusions

419

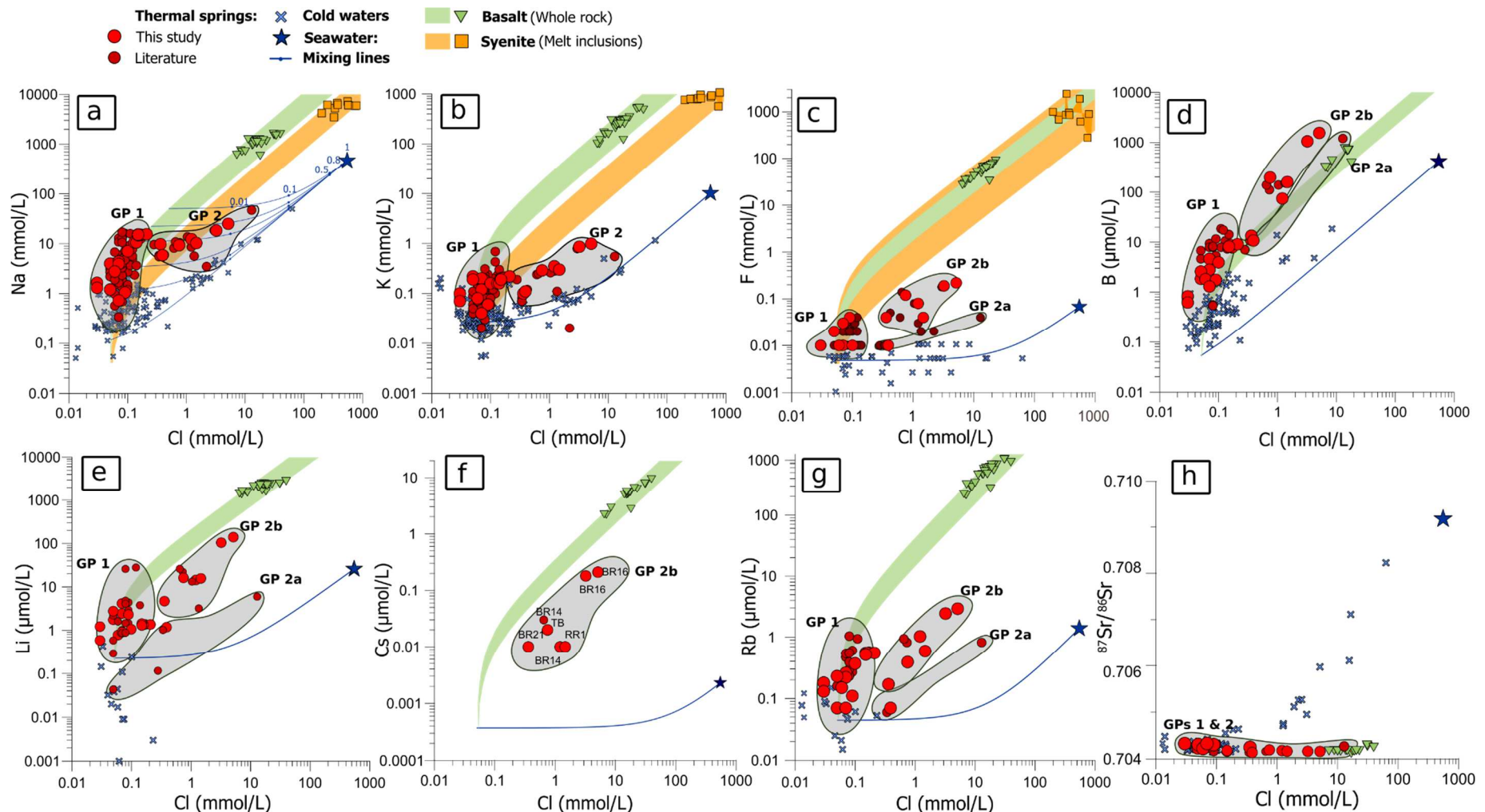
#### 420 *Strontium isotopes*

421 Our classification of Piton des Neiges thermal springs into three groups, summarized in Table  
 422 4, may be compared with isotope data which provide additional information about the relative  
 423 contribution of each pool to the mineralization of spring waters. Among them, the  $^{87}\text{Sr}/^{86}\text{Sr}$  ratio  
 424 is a good tracer of water-rock interaction or seawater contamination. The narrow range of  
 425  $^{87}\text{Sr}/^{86}\text{Sr}$  values obtained for spring waters (0.704142 to 0.704336), irrespective of Cl  
 426 concentration and consistent with Piton des Neiges volcanic rocks (0.704041 to 0.704368),  
 427 clearly indicates that strontium concentration is buffered by water-rock interaction in all the  
 428 thermal springs of Groups 1 and 2 (Figure 5h). This  $^{87}\text{Sr}/^{86}\text{Sr}$  signature contrasts with that of cold  
 429 waters, increasingly influenced by seawater (0.709179) at increasing [Cl] (Figure 5h). It is thus  
 430 manifest that seawater contamination is too limited to affect the Sr isotopic signature of thermal  
 431 springs, no matter their group.

#### 432 *Lithium isotopes*

433      The  $\delta^7\text{Li}$  signature of waters is used as a tracer of hydrothermal alteration and water-rock  
434 interaction. At Piton des Neiges, the lowest lithium concentration is found in a surface water from  
435 the Ferrière river in Cilaos (RFER), whose  $\delta^7\text{Li}$  of +25.2 ‰ is interpreted as reflecting the  
436 isotopic signature of rain water. Group 1 thermal springs display decreasing  $\delta^7\text{Li}$  values from  
437 +16.6 to +7.5 ‰ with increasing lithium concentration (Figure 6a; Table 4). Given the  $\delta^7\text{Li}$   
438 range of Réunion basalts (+3.9 to +4.4 ‰, Krienitz et al., 2012), this decreasing trend suggests,  
439 in agreement with element analyses (Figure 5), that Group 1 springs results from meteoric water  
440 interaction with basaltic rocks, as documented in pore waters leaching basalts from Iceland,  
441 Hawaii or the Columbia River (Liu et al., 2015, 2013; Pogge von Strandmann et al., 2012; Ryu et  
442 al., 2014). The two samples from Salazie rivers (RBACH and RMAT) mimic the decreasing trend  
443 at lower [Li], probably because these streams collect springs belonging to Group 1.

444      Lithium isotopes are also convenient to identify contamination by seawater due to its high  $\delta^7\text{Li}$   
445 (+31 ‰), or by magmatic inputs due to their negative  $\delta^7\text{Li}$  ( $\leq -1.3$  ‰ at Piton de la Fournaise  
446 (Vlastélic et al., 2011). At increasing lithium concentration, Group 2a springs (BB, sRMAT3 and  
447 OLIV2) show an increasing  $\delta^7\text{Li}$  trend (up to +34.8 ‰) with increasing [Li]. As for Na vs Cl or K  
448 vs Cl diagrams (Figure 5 a-b), we interpret this increasing  $\delta^7\text{Li}$  trend as an influence of seawater  
449 in Group 2a, the most contaminated spring being OLIV2 (Table 4). Group 2b springs (OLIV1,  
450 BR12) fall at the high [Li], low  $\delta^7\text{Li}$  end of the meteoric water / rock interaction trend, with BR12  
451 showing the lowest  $\delta^7\text{Li}$  value of our dataset (+2 ‰). This low value cannot be accounted for by  
452 water interaction basalt because it is below the range of available data for La Réunion basalts  
453 (+3.9 and 4.4 ‰). At Piton de la Fournaise, Vlastélic et al. (2011) have shown that degassing-  
454 induced Li fractionation during magma differentiation could produce very light lithium  
455 compositions in fumarolic deposits ( $-2.8 \leq \delta^7\text{Li} \leq -1.3$  ‰), and even lighter lithium compositions  
456 in differentiated (trachytic) melts ( $-21 \leq \delta^7\text{Li} \leq -17$  ‰). As for element ratios in Group 2 springs  
457 (Figure 5c-g), we conclude that the low  $\delta^7\text{Li}$  signature of BR12 is thus either compatible with  
458 leaching of a very differentiated rock, or with the incorporation of depleted lithium from  
459 magmatic gas or fumarolic deposits.

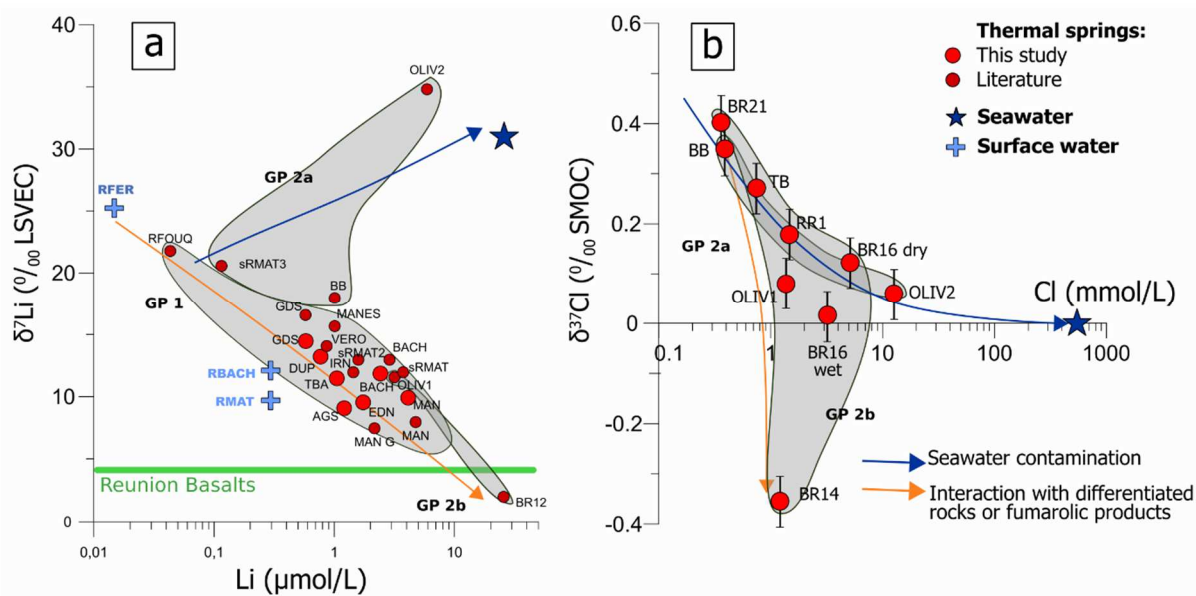


460

461 Figure 5: Comparison of Na, K, F, B, Li, Cs, Rb,  $^{87}\text{Sr}/^{86}\text{Sr}$  vs Cl molar concentrations for Piton des Neiges thermal springs with cold waters (rivers and groundwater), seawater  
 462 and mafic and differentiated rocks (basalt whole rock and melt inclusions from syenite, respectively) from Réunion. Literature data are from (Aunay et al., 2013, 2012; Aunay  
 463 and Gourcy, 2007; Belle, 2014; Frissant et al., 2005, 2003; Iundt et al., 1992; Lopoukhine and Stieltjes, 1978; Louvat and Allègre, 1997; Nauret et al., 2019; Petit et al., 2013a,  
 464 2013b; Rogers et al., 2012; Sanjuan et al., 2001; Smietana, 2011; Vigouroux et al., 2009; Vlastélic et al., 2013, 2007, 2005; Welsch et al., 2013)). Thermal springs can be  
 465 subdivided into three groups according to their chemical composition. Error bars are shorter than symbols.

466 *Chlorine isotopes*

467  $\delta^{37}\text{Cl}$  represents a promising geochemical tool under development to track the origin of Cl in  
 468 hydrothermal fluids. Because of the  $\sim 10 \text{ mg/L}$  analytical limit, all the springs analyzed for  $\delta^{37}\text{Cl}$   
 469 belong to Group 2. Both Groups 2a and 2b show a clear mixing trend of decreasing  $\delta^{37}\text{Cl}$  from  
 470  $+0.4 \text{ ‰}$  at low Cl concentration, to seawater at  $0 \text{ ‰}$  at high Cl concentration, except for BR14  
 471 from Group 2b that stands out with a negative  $\delta^{37}\text{Cl}$  value of  $-0.4 \text{ ‰}$  (Figure 6b). To compare  
 472 these data with the still limited database of worldwide chlorine isotope analyses, we chose those  
 473 coming from the same laboratory in order to avoid inter-laboratory comparisons. In this even  
 474 more restricted dataset, tropical ocean island rainwater fall in the range of  $-0.17$  to  $0.38 \text{ ‰}$ ,  
 475 whereas mantle magmas and arc magmas are thought to display rather negative average  $\delta^{37}\text{Cl}$   
 476 values ( $-3.0$  to  $-0.2 \text{ ‰}$ , see Li et al., (2015) for a review and discussion). In consequence, we  
 477 interpret the  $+0.4 \text{ ‰}$   $\delta^{37}\text{Cl}$  signature of low-chlorinity springs, such as BR21 (Group 2b), as  
 478 reflecting the signal of rainwater. As in other spaces, OLIV2 (Group 2a), the most Cl enriched  
 479 spring of La Réunion, is also the one showing the greatest  $\delta^{37}\text{Cl}$  influence of seawater (at  $0 \text{ ‰}$ )  
 480 with a  $\delta^{37}\text{Cl}$  of  $0.06 \text{ ‰}$ . As shown by other tracers, the negative  $\delta^{37}\text{Cl}$  of spring BR14 in Group 2b  
 481 ( $-0.4 \text{ ‰}$ ) is consistent with a magmatic origin. The two data for spring BR16 (also Group 2b)  
 482 suggest that the wet season drags Cl concentration and  $\delta^{37}\text{Cl}$  toward lower values, perhaps  
 483 because the water recharge flushes seawater downward in the island, thus enhancing the  
 484 contribution of magmatic Cl. The spring OLIV1 (Group 2a) might also be influenced by this  
 485 magmatic input. From these data, we infer that Cl is mostly of marine origin for all the springs of  
 486 Group 2, with a small magmatic contribution essentially apparent in Group 2b (Table 4).



487

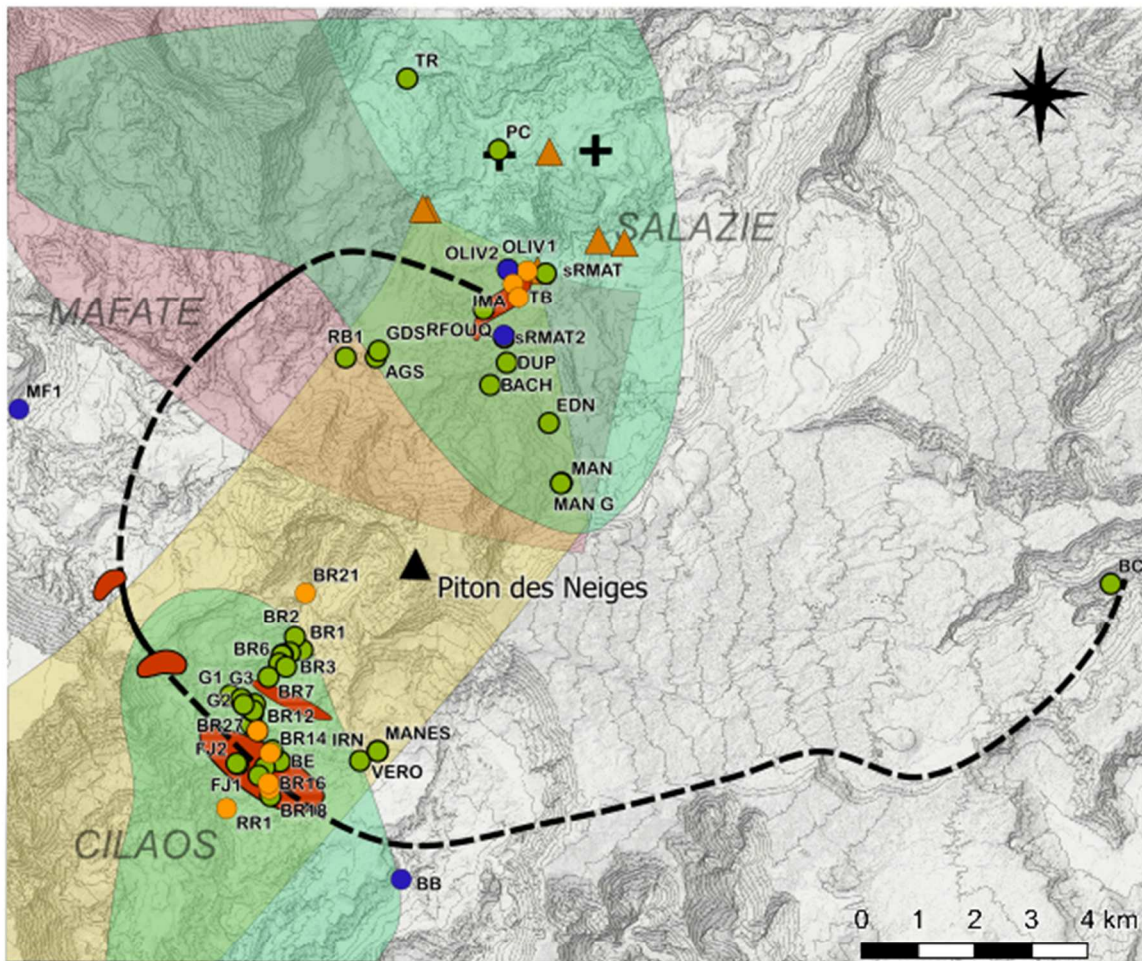
488 Figure 6: (a)  $\delta^7\text{Li}$  vs Li concentration, and (b)  $\delta^{37}\text{Cl}$  vs Cl concentration for waters of Piton des Neiges.  $\delta^7\text{Li}$  and  
 489  $\delta^{37}\text{Cl}$  show two trends, one toward seawater, the other one toward dissolution of a very differentiated rock, of  
 490 magmatic gas or of fumarolic deposits.  $\delta^7\text{Li}$  error bars are shorter than symbols.

491      *Sulfur isotopes*

492      Literature sulfur isotopes data bring further support to our interpretation of seawater and  
493 fumarolic inputs in Piton des Neiges hydrothermal system (Table 4). Indeed, (Sanjuan et al.,  
494 2001) report nine  $\delta^{34}\text{S}_{\text{SO}_4}$  analyses of thermal springs enriched in sulfates. One of them, the  
495 spring OLIV2 belonging to Group 2a, displays a high  $\delta^{34}\text{S}_{\text{SO}_4}$  at +8.9 ‰, consistent with a slight  
496 contamination of this spring by  $\text{SO}_4$  from seawater (at  $\delta^{34}\text{S}_{\text{SO}_4}=20\text{ ‰}$ ). The eight other springs,  
497 belonging to Groups 1 and 2, have  $\delta^{34}\text{S}_{\text{SO}_4}$  values between +2.0 and +5.8 ‰, consistent with  
498 the signature of  $\text{SO}_4$  degassed from a basaltic melt (+2 ‰). In the study area, there is evidence  
499 of fossil and active fumarolic sulfide deposits (Lopoukhine and Steltjes, 1978; Rançon and  
500 Rocher, 1985). Like other volatile species, dissolved  $\text{SO}_4$  may thus come from the dissolution of  
501 magmatic gas or from the oxidation of magmatic sulfur condensates.

502      *Spatial repartition*

503      Most of the thermal springs (Groups 1 and 2) and other hydrothermal indicators are located at  
504 the intersection of two or three of the preferential magma intrusion zones (the N030-040 and  
505 N120-160 rift zones and/or a sill zone), suggesting that the junctions of these intrusion zones are  
506 more favorable to geothermal activity (Figure 7). However, the majority of thermal springs also  
507 occur within the perimeter of the proposed caldera associated with the terminal stage of Piton  
508 des Neiges activity. It is thus not possible to determine which structure is the primary pathway  
509 for geothermal fluid circulation. Nevertheless, two other important features of spatial repartition  
510 become apparent when thermal springs are plotted according to our group subdivision (Table 4):  
511 (1) Group 2a springs are restricted to the outer rim of the hydrothermal system, outside the  
512 proposed caldera of the terminal volcanic stage, and (2) Group 2b are located in the vicinity of  
513 the major syenite intrusions interpreted as delineating the caldera. The first observation suggests  
514 that the proposed caldera, if it does exist, acts as a hydrological barrier isolating the inner part of  
515 the hydrothermal system from seawater contamination. The second observation designates  
516 syenite dykes as possible candidates responsible for the interaction of Group 2b springs with  
517 highly differentiated rocks or magmatic gas.



#### Thermal springs

- Interaction with basalts  
= Group 1
- + Seawater contamination  
= Group 2a
- + Interaction with differentiated rocks or fumarolic products  
= Group 2b

- Sill zones
- Rift zone N30°E
- Rift zone N110-160°E

- Deep boreholes
- Sulfide deposits
- Caldera
- Syenite intrusions

518

519 Figure 7: Map of the thermal springs of Piton des Neiges, classified in three groups according to mineralization  
 520 processes from their geochemical profiles in major trace elements,  $\delta^7\text{Li}$  and  $\delta^{37}\text{Cl}$  values. Map in UTM coordinates  
 521 (EPSG:2975, RGR92 / UTM 40s, relief contours at 100 m intervals) from RGE ALTI® - IGN.

522

523     5.4. Architecture of hydrothermal circulation

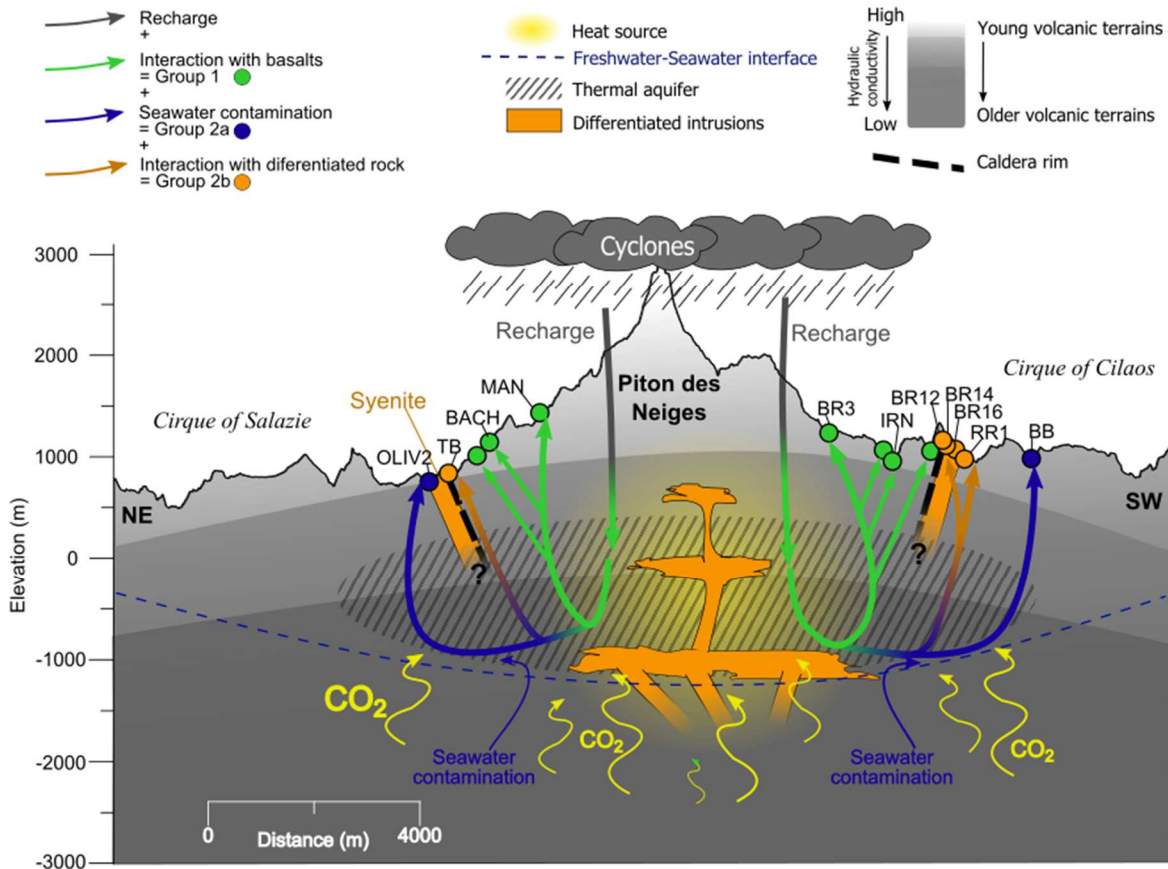
524     Our new chemical analyses, combined with literature data, may be used to bring constraints  
 525 on the geometry of Piton des Neiges' hydrothermal system, as illustrated in Figure 8. A first  
 526 important constraint is that water, carbon and other dissolved species are provided by  
 527 independent pools. Cyclones or heavy rains and/or high altitude rainfalls that penetrate into the  
 528 volcanic edifice are the main contributors to the recharge of the thermal aquifer. Carbon is of

529 primary magmatic origin and dissolves in the thermal aquifer. Three independent pools contribute  
530 to the other species dissolved in thermal waters: 1) interaction with basalt at temperature  $\geq$ 50  
531 °C for all the springs (Groups 1 and 2 springs) enhanced by dissolved CO<sub>2</sub>, 2) slight seawater  
532 contamination on the outer rim of the hydrothermal system, possibly delimited by a caldera  
533 (Group 2a), and/or 3) interaction with a differentiated rock such as syenite, or dissolution of  
534 magmatic gas or fumarolic deposits (Group 2b).

535 Where is the magma at the origin of carbon discharge in hydrothermal waters located? The  
536 solubility of carbon in silicate melts is very low compared to other volatile species (e.g. H<sub>2</sub>O, S,  
537 Cl.). This solubility decreases with decreasing pressure, and thus with the ascent of magmas.  
538 Starting from a mantle carbon composition, a rising basaltic melt loses about 80% of its CO<sub>2</sub>  
539 before entering the Réunion edifice at  $\sim$ 7 km depth (Di Muro et al., 2016). The source of  
540 magmatic carbon can thus be located at any depth from the base of the island to the upper  
541 mantle. In Réunion Island, seismic crises at 10 – 20 km depth have been correlated with spikes  
542 of soil carbon fluxes and concentration at the surface (Boudoire et al., 2017). This suggests that  
543 carbon degassing and ascent occurs at the scale of the whole island, from a magmatic source  
544 located in the oceanic crust or in the mantle. Thermal springs have also a mantle helium isotopic  
545 signature (Marty et al., 1993; Trull et al., 1993). Therefore, it is more probable that the TDIC of  
546 thermal waters is supplied by deep regional degassing of the Réunion hot spot rather than by a  
547 shallow magma within Piton des Neiges volcano. Carbon is mixed with thermal waters during its  
548 ascent toward the surface.

549 On the other hand, elements like S, Cl, F, and perhaps B, Li, Rb, and Cs are much more  
550 soluble volatile species than CO<sub>2</sub> in silicate melts, and degas at low pressure in the case of  
551 basaltic liquids (0 – 200 MPa). The source of these volatile or semi-volatile elements in Group 2b  
552 springs is either a degassing magma or an accumulation of fossil condensates deposited by  
553 former degassing. It is located at shallow depth within the volcanic edifice (0 – 7 km depth), and  
554 is independent from the carbon supply.

555

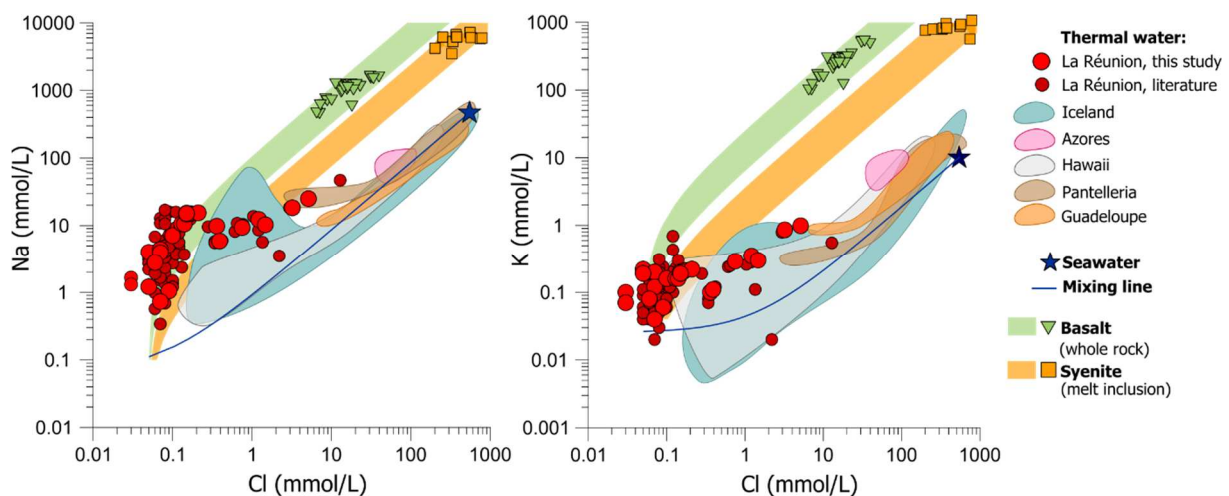


557 Figure 8: Conceptual model of Piton des Neiges' hydrothermal system. Meteoric water from cyclones  
 558 and heavy rains penetrates in the edifice and is heated by intrusions of the terminal activity of the volcano.  
 559 Magmatic CO<sub>2</sub> from regional extent degassing mixes with thermal water and increases its acidity.  
 560 Temperature and acidity enhance water-rock interaction with the basaltic edifice, as recorded in all the springs.  
 561 Group 1 springs are entirely mineralized by this process. Group 2 springs show an additional source of  
 562 mineralization by slight seawater contamination (< 3 mol%). Seawater contamination is most apparent in  
 563 springs from the outer parts of the hydrothermal system (Group 2a), possibly delimited by a caldera.  
 564 A few springs, located near syenite intrusions associated with the terminal activity of the volcano,  
 565 are also mineralized by interaction with a differentiated rock (like the syenite) or with volatiles exsolved from a differentiated magma.

566

567 The heat source of the hydrothermal system is neither the source of carbon nor of other  
 568 volatile elements, because springs interact with rocks no matter their concentration in C, S, Cl, F,  
 569 B, Li, Rb, and Cs. This inference has to be put in parallel with the low contamination of the  
 570 hydrothermal system by seawater, only found as a low contribution (<3 mol%, Group 2a) in the  
 571 lowermost and outermost springs of Piton des Neiges. By comparison, seawater is the dominant  
 572 water source in most hydrothermal systems from other ocean island volcanoes such as  
 573 Pantelleria, Azores and Guadeloupe (Carvalho et al., 2006; Gianelli and Grassi, 2001; Sanjuan et  
 574 al., 1999). Even in geothermal systems alimented by meteoric such as Krafla in Iceland and Maui  
 575 in Hawaii (Arnórsson, 1995a; Thomas, 1984), Cl enrichment is seldom as low as for the Group 1  
 576 thermal springs of Piton des Neiges (Fig. 9). The hydrothermal system of Piton des Neiges is thus  
 577 exceptionally isolated from seawater compared with the above examples. This exceptional  
 578 isolation may be explained by the conjunction of several factors. First, the hydrothermal system,

579 as viewed from thermal springs, is likely protected from seawater by hydrological barriers such as  
 580 intrusions, faults, or low-permeability layers. In particular, structural studies emphasize the  
 581 abundance of sills at Piton des Neiges (Chaput et al., 2017, 2014), which may prevent any  
 582 vertical transport of seawater. The spatial repartition of Group 2 springs suggests that the syenite  
 583 dykes and/or the terminal caldera of the volcano may also act as hydrological barriers isolating  
 584 the hydrothermal system. In addition, pore clogging by minerals of the phrenite-pumpellyite  
 585 facies occurs in all the units older than 640 ka that constitute the basement of Piton des Neiges  
 586 (Chevalier, 1979; Chovelon, 1968; Famin et al., 2016; Join et al., 2016). However, secondary  
 587 mineral precipitation also occurs in Hawaii and the Azores (Cruz, 2003; Izquierdo, 2014;  
 588 Schiffman et al., 2006) and thus hardly explains alone the isolation of the hydrothermal system  
 589 from seawater in our case. Another hypothesis is that the strong input of meteoric water  
 590 increases the hydraulic head in the center of the massif, thus lowering the freshwater/seawater  
 591 interface and flushing seawater outward and downward. Réunion Island has higher precipitation  
 592 rates than Pantelleria, Iceland or the Azores, but not than Hawaii or Guadeloupe, which calls for  
 593 an additional factor. At Piton de la Fournaise, in many respects considered as an active analogue  
 594 of Piton des Neiges, the uppermost magma reservoir feeding most of the eruption is located at 0  
 595 to +500 m (Peltier et al., 2008). Following this analogy, we suggest the hydrothermal system of  
 596 Piton des Neiges is isolated from seawater because its heat source is located at or above sea  
 597 level, in conjunction with being protected by low permeability barriers and an intense supply of  
 598 freshwater under tropical climate.



599

600 Figure 9: Comparison of Na and K vs Cl molar concentrations for Piton des Neiges thermal springs with thermal  
 601 water from Iceland, Azores, Hawaii, Pantelleria, Guadeloupe, and with seawater and rocks from Réunion.  
 602 Literature data are from Arnórsson (1995a, 1995b), Belle (2014), Boivin and Bachélery (2009), Carvalho et al.  
 603 (2006), Fretzdorff and Haase (2002), Frissant et al. (2003), Gianelli and Grassi (2001), Iundt et al. (1992),  
 604 Lopoukhine and Stieljes (1978), Louvat and Allègre (1997), Sanjuan et al. (2001, 1999), Smietana (2011),  
 605 Thomas (1984), Vigouroux et al. (2009), Vlastélic et al. (2013, 2007, 2005), Welsch et al. (2013). Compared to  
 606 other geothermal systems in oceanic islands, the hydrothermal system of Piton des Neiges is exceptionally  
 607 disconnected from seawater.

Our preferred model of hydrothermal circulation has implications for the future of geothermal prospection at Piton des Neiges. In particular, the isolation of thermal waters from seawater is a promising clue that the heat source may be reached by drilling depths of ~1000 m (i.e. sea level), if boreholes are implanted in the cirques at +1000 m. This drilling depth is similar to that of maximum temperature in Pantelleria (Fulignati et al., 1997) and twice less than the depth of the Krafla geothermal field in Iceland (Arnórsson, 1995a). On the other hand, this isolation also implies that production might be limited by the meteoric recharge. In this respect, time series of stable isotopes analyses will be necessary to determine if thermal springs fluctuate in tandem with cyclonic precipitation (i.e. small aquifer) or are steady in time (aquifer large enough to be buffered by long-term recharge). Our study also shows that thermal waters interact with differentiated rocks and/or with volatiles or fumarolic deposits degassed from shallow differentiated magmas. Again, this situation is very similar to that of Pantelleria, for which the hydrothermal system is related to syenite intrusions in the vicinity of caldera faults. Future prospection should thus focus on the spatial repartition of differentiated intrusions and hot springs, taking into account their chemistry to identify pathways of preferential circulation. The occurrence of volatiles species degassed from shallow magmas in springs also questions the age of the last intrusive activity of Piton des Neiges, which might be considerably younger than its terminal eruption at 12, 22 or 29 ka.

## 6. Conclusion

By combining major/trace element chemistry with a large number of isotopic tools (O, H, C, Sr, Li, Cl), our study untangles the complex history of fluid mixing from multiple pools at the origin of Piton des Neiges' hydrothermal system. Water is of meteoric origin, principally supplied by cyclones and/or high altitude precipitation, with no significant contribution from either rivers or cold groundwater. Unlike in many ocean island volcanoes, seawater does not participate in the recharge feeding the thermal springs, except as a slight contaminant at the external rim of the hydrothermal system. Thermal water is mixed with magmatic carbon, probably originating from regional mantle degassing, and interacts with basaltic rocks at temperatures  $\geq 50$  °C. The absence of  $^{18}\text{O}$  enrichment of the thermal waters relative to local groundwaters indicates that their oxygen isotope exchange with rocks is limited, and therefore suggests that their temperatures of interaction are relatively low (<180 °C) and/or that waters buffer the oxygen isotope composition of rocks. Higher-than-seawater B/Cl, F/Cl, Cs/Cl, Li/Cl and Rb/Cl ratios as well as low Li and Cl isotopic ratios suggest that some thermal waters also dissolve magmatic gases or fumarolic deposits exsolved from shallow (intra-edifice) differentiated trachytic melts. Whether this input corresponds to an active magma reservoir or to fossil evaporites remains uncertain.

Our study provides insights on the architecture of the hydrothermal system of key importance for future geothermal exploration. Thermal waters are protected from shallow aquifers by low-porosity barriers, and their recharge occurs mostly during exceptional rain events. The noteworthy lack of seawater in the hydrothermal system, exceptional for this kind of geological environments, implies that convection cells are located above the seawater/freshwater interface. The heat source, of trachytic nature and disconnected from the magmatic carbon source, may thus be reached within reasonable drilling depths ( $\leq 1000$  m). These results may serve as a basis to design the next step of geothermal exploration, oriented toward estimating the maximum temperature of the deep geothermal waters (using solute chemical and isotope geothermometers integrated into a multicomponent modelling approach) and the size of the hydrothermal reservoir.

## 7. Acknowledgments

We thank Jonas Greve and Victor K/Bidi for their participation in the fieldwork and the Établissement thermal de Cilaos for giving us access to their facilities and resources. The Ph.D. fellowship of B. Bénard is funded by Le Conseil Régional de La Réunion. We thank also B. Minster for her help in the analysis of water isotope ratios. The  $\delta^7\text{Li}$  analyses from 2001 were performed by R. Millot (BRGM) within the framework of the ADEME-BRGM project GHEDOM. This research has been supported by INSU-CNRS and OSU-Réunion grants, by EDENA, and by IPGP multidisciplinary program PARI and Paris–IdF region SESAME (Grant no. 12015908). This is IPGP contribution XXXX

## 8. References

- Adams, M.C., 1996. Chemistry of fluids from ascension #1, a deep geothermal well on ascension island, South Atlantic Ocean. *Geothermics, Geothermal Exploration on Ascension Island* 25, 561–579. [https://doi.org/10.1016/0375-6505\(96\)00011-9](https://doi.org/10.1016/0375-6505(96)00011-9)
- Arnórsson, S., 1995a. Geothermal systems in Iceland: Structure and conceptual models—I. High-temperature areas. *Geothermics* 24, 561–602. [https://doi.org/10.1016/0375-6505\(95\)00025-9](https://doi.org/10.1016/0375-6505(95)00025-9)
- Arnórsson, S., 1995b. Geothermal systems in Iceland: Structure and conceptual models—II. Low-temperature areas. *Geothermics* 24, 603–629. [https://doi.org/10.1016/0375-6505\(95\)00026-7](https://doi.org/10.1016/0375-6505(95)00026-7)
- Assayag, N., Rivé, K., Ader, M., Jézéquel, D., Agrinier, P., 2006. Improved method for isotopic and quantitative analysis of dissolved inorganic carbon in natural water samples. *Rapid Commun. Mass Spectrom.* 20, 2243–2251. <https://doi.org/10.1002/rcm.2585>
- Aunay, B., Dewandel, B., Ladouce, B., Oliva, Z., Saussol, P., 2012. Identification des modalités d'exploitation des ressources en eaux souterraines du domaine d'altitude de l'Est de La Réunion – Phase 3 (secteur des Plaines) (No. RP-59245-FR <http://infoterre.brgm.fr/rapports/RP-59245-FR.pdf>). BRGM.
- Aunay, B., Gourcy, L., 2007. Approche hydrogéochimique pour la détermination de l'origine de la contamination des eaux. (No. RP-55535-FR <http://infoterre.brgm.fr/rapports//RP-55535-FR.pdf>). BRGM.

- 683 Aunay, B., Lucas, C., Ladouche, B., Vigouroux, P., Belle, P., 2013. Identification du potentiel en  
684 eau minérale gazeuse du cirque de Salazie (No. RC-62181-FR). BRGM.
- 685 Belle, P., 2014. Contribution des processus hydrologiques et hydrogéologiques aux glissements  
686 de terrain de grande ampleur. Application au contexte tropical de La Réunion. Université  
687 de La Réunion, Saint-Denis, La Réunion.
- 688 Bertani, R., 2005. World geothermal power generation in the period 2001–2005. *Geothermics* 34,  
689 651–690. <https://doi.org/10.1016/j.geothermics.2005.09.005>
- 690 Boivin, P., Bachèlery, P., 2009. Petrology of 1977 to 1998 eruptions of Piton de la Fournaise, La  
691 Réunion Island. *J. Volcanol. Geotherm. Res., Recent advances on the geodynamics of*  
692 *Piton de la Fournaise volcano* 184, 109–125.  
693 <https://doi.org/10.1016/j.jvolgeores.2009.01.012>
- 694 Bonifacie, M., Monnin, C., Jendrzejewski, N., Agrinier, P., Javoy, M., 2007. Chlorine stable  
695 isotopic composition of basement fluids of the eastern flank of the Juan de Fuca Ridge  
696 (ODP Leg 168). *Earth Planet. Sci. Lett.* 260, 10–22.  
697 <https://doi.org/10.1016/j.epsl.2007.05.011>
- 698 Boudoire, G., Liuzzo, M., Di Muro, A., Ferrazzini, V., Michon, L., Grassa, F., Derrien, A.,  
699 Villeneuve, N., Bourdeu, A., Brunet, C., Giudice, G., Gurrieri, S., 2017. Investigating the  
700 deepest part of a volcano plumbing system: Evidence for an active magma path below  
701 the western flank of Piton de la Fournaise (La Réunion Island). *J. Volcanol. Geotherm.*  
702 *Res.* 341, 193–207. <https://doi.org/10.1016/j.jvolgeores.2017.05.026>
- 703 Boudoire, G., Rizzo, A.L., Di Muro, A., Grassa, F., Liuzzo, M., 2018. Extensive CO<sub>2</sub> degassing in  
704 the upper mantle beneath oceanic basaltic volcanoes: First insights from Piton de la  
705 Fournaise volcano (La Réunion Island). *Geochim. Cosmochim. Acta* 235, 376–401.  
706 <https://doi.org/10.1016/j.gca.2018.06.004>
- 707 Carvalho, M.R., Forjaz, V.H., Almeida, C., 2006. Chemical composition of deep hydrothermal  
708 fluids in the Ribeira Grande geothermal field (São Miguel, Azores). *J. Volcanol. Geotherm.*  
709 *Res.* 156, 116–134. <https://doi.org/10.1016/j.jvolgeores.2006.03.015>
- 710 Chaput, M., Famin, V., Michon, L., 2017. Sheet intrusions and deformation of Piton des Neiges,  
711 and their implication for the volcano-tectonics of La Réunion. *Tectonophysics* 717, 531–  
712 546. <https://doi.org/10.1016/j.tecto.2017.08.039>
- 713 Chaput, M., Pinel, V., Famin, V., Michon, L., Froger, J.-L., 2014. Cointrusive shear displacement  
714 by sill intrusion in a detachment: A numerical approach. *Geophys Res Lett* 41 1937–1943.
- 715 Chevalier, L., 1979. Structures et évolution du volcan Piton des Neiges. Ile de la Réunion. Leurs  
716 relations avec les structures du bassin des Mascareignes. Océan indien occidental  
717 (Thèse). Université scientifique et médicale de Grenoble.
- 718 Chovelon, P., 1968. Forage géothermique de Salazie (SLZ1). Étude géologique du forage et  
719 dossier des ouvrages exécutés. (No. N°86CFG018).
- 720 Cruz, J.V., 2003. Groundwater and volcanoes: examples from the Azores archipelago. *Environ.*  
721 *Geol.* 44, 343–355. <https://doi.org/10.1007/s00254-003-0769-2>
- 722 Deines, P., 2002. The carbon isotope geochemistry of mantle xenoliths. *Earth-Sci. Rev.* 58, 247–  
723 278. [https://doi.org/10.1016/S0012-8252\(02\)00064-8](https://doi.org/10.1016/S0012-8252(02)00064-8)
- 724 Delibrias, G., Guillier, M.-T., Labeyrie, J., 1986. Gif Natural Radiocarbon Measurements X.  
725 *Radiocarbon* 28, 9–68. <https://doi.org/10.1017/S0033822200060008>
- 726 Deniel, C., Kieffer, G., Lecointre, J., 1992. New 230Th-238U and 14C age determinations from  
727 Piton des Neiges volcano, Reunion — A revised chronology for the Differentiated Series.  
728 *J. Volcanol. Geotherm. Res.* 51, 253–267. [https://doi.org/10.1016/0377-0273\(92\)90126-X](https://doi.org/10.1016/0377-0273(92)90126-X)
- 729 Dezayes, C., Baltassat, J.M., Famin, V., Bes de Berc, S., 2016. Potential interest areas for the  
730 development of geothermal energy in La Reunion Island. Presented at the European  
731 Geothermal Congress, Strasbourg, France.
- 732 Di Muro, A., Métrich, N., Allard, P., Aiuppa, A., Burton, M., Galle, B., Staudacher, T., 2016.  
733 Magma Degassing at Piton de la Fournaise Volcano, in: Active Volcanoes of the  
734 Southwest Indian Ocean, Active Volcanoes of the World. Springer, Berlin, Heidelberg, pp.  
735 203–222. [https://doi.org/10.1007/978-3-642-31395-0\\_12](https://doi.org/10.1007/978-3-642-31395-0_12)
- 736 Druecker, M., Fan, P., 1976. Hydrology and Chemistry of Ground Water a in Puna, Hawaiiia.  
737 *Groundwater* 14, 328–338. <https://doi.org/10.1111/j.1745-6584.1976.tb03123.x>

- 738 Eggenkamp, H.G.M., Middelburg, J.J., Kreulen, R., 1994. Preferential diffusion of  $^{35}\text{Cl}$  relative to  
739  $^{37}\text{Cl}$  in sediments of Kau Bay, Halmahera, Indonesia. *Chem. Geol.* 116, 317–325.  
740 [https://doi.org/10.1016/0009-2541\(94\)90022-1](https://doi.org/10.1016/0009-2541(94)90022-1)
- 741 Famin, V., Berthod, C., Michon, L., Eychenne, J., Brothelande, E., Mahabot, M.-M., Chaput, M.,  
742 2016. Localization of magma injections, hydrothermal alteration, and deformation in a  
743 volcanic detachment (Piton des Neiges, La Réunion). *J. Geodyn.*, Fluids in crustal  
744 deformation: fluid flow, fluid-rock interactions, rheology, melting and resources 101,  
745 155–169. <https://doi.org/10.1016/j.jog.2016.05.007>
- 746 Fretzdorff, S., Haase, K.M., 2002. Geochemistry and petrology of lavas from the submarine flanks  
747 of Réunion Island (western Indian Ocean): implications for magma genesis and the  
748 mantle source. *Mineral. Petrol.* 75, 153–184. <https://doi.org/10.1007/s007100200022>
- 749 Frissant, N., Gourcy, L., Brach, M., 2005. Recherche d'une relation entre le plateau de Dos-d'Ane  
750 et les sources Blanche et Denise (No. RP-54167-FR <http://infoterre.brgm.fr/rapports/RP-54167-FR.pdf>). BRGM.
- 751 Frissant, N., Lacquement, F., Rançon, J.P., 2003. Etude du potentiel hydrothermal de la zone  
752 amont de la rivière du Bras Rouge (Cirque de Cilaos) -Première phase d'étude- (No. RP-  
753 52673-FR <http://infoterre.brgm.fr/rapports/RP-52673-FR.pdf>). BRGM.
- 754 Fulignati, P., Malfitano, G., Sbrana, A., 1997. The Pantelleria caldera geothermal system: Data  
755 from the hydrothermal minerals. *J. Volcanol. Geotherm. Res.* 75, 251–270.  
756 [https://doi.org/10.1016/S0377-0273\(96\)00066-2](https://doi.org/10.1016/S0377-0273(96)00066-2)
- 757 Gianelli, G., Grassi, S., 2001. Water–rock interaction in the active geothermal system of  
758 Pantelleria, Italy. *Chem. Geol.* 181, 113–130. [https://doi.org/10.1016/S0009-2541\(01\)00276-5](https://doi.org/10.1016/S0009-2541(01)00276-5)
- 759 Gillot, P.-Y., Nativel, P., 1982. K-Ar chronology of the ultimate activity of piton des neiges  
760 volcano, reunion island, Indian ocean. *J. Volcanol. Geotherm. Res.* 13, 131–146.  
761 [https://doi.org/10.1016/0377-0273\(82\)90024-5](https://doi.org/10.1016/0377-0273(82)90024-5)
- 762 Godon, A., Jendrzejewski, N., Eggenkamp, H.G.M., Banks, D.A., Ader, M., Coleman, M.L., Pineau,  
763 F., 2004. A cross-calibration of chlorine isotopic measurements and suitability of seawater  
764 as the international reference material. *Chem. Geol.* 207, 1–12.  
765 <https://doi.org/10.1016/j.chemgeo.2003.11.019>
- 766 Gourcy, L., Renaud, T., Aunay, B., 2018. Etude des modes de transfert et de l'origine des nitrates  
767 sur les secteurs de La Saline-l'Hermitage (FRH5) et de Dos d'Ane (Galets Ronds). (No.  
768 RP-66338-FR <http://infoterre.brgm.fr/rapports/RP-66338-FR.pdf>). BRGM.
- 769 Grunberger, O., 1989. Etude géochimique et isotopique de l'infiltration sous climat tropical  
770 contrasté. Massif du Piton des Neiges. Ile de la Réunion (Thèse). Université de Paris XI.
- 771 Guilpart, E., Vimeux, F., Evan, S., Brioude, J., Metzger, J.-M., Barthe, C., Risi, C., Cattani, O.,  
772 2017. The isotopic composition of near-surface water vapor at the Maïdo observatory  
773 (Reunion Island, southwestern Indian Ocean) documents the controls of the humidity of  
774 the subtropical troposphere. *J. Geophys. Res. Atmospheres* 122, 9628–9650.  
775 <https://doi.org/10.1002/2017JD026791>
- 776 Hoefs, J., 2015. Stable Isotope Geochemistry. Springer.
- 777 Iundt, F., Mauroux, B., Barrera, L., Cruchet, M., Martignoni, P., Stieltjes, L., 1992. Etude des  
778 sources thermominérales de Cilaos (No. RR-35833-FR). BRGM.
- 779 Izquierdo, T., 2014. Conceptual hydrogeological model and aquifer system classification of a  
780 small volcanic island (La Gomera; Canary Islands). *CATENA* 114, 119–128.  
781 <https://doi.org/10.1016/j.catena.2013.11.006>
- 782 Johnston, J.M., Pellerin, L., Hohmann, G.W., 1992. Evaluation of Electromagnetic Methods for  
783 Geothermal Reservoir Detection. *Geotherm. Resour. Counc. Trans.* 16, 241–245.
- 784 Join, J.-L., Folio, J.-L., Bourhane, A., Comte, J.-C., 2016. Groundwater Resources on Active  
785 Basaltic Volcanoes: Conceptual Models from La Réunion Island and Grande Comore, in:  
786 Bachelery, P., Lenat, J.-F., Di Muro, A., Michon, L. (Eds.), *Active Volcanoes of the*  
787 *Southwest Indian Ocean*. Springer Berlin Heidelberg, Berlin, Heidelberg, pp. 61–70.  
788 [https://doi.org/10.1007/978-3-642-31395-0\\_5](https://doi.org/10.1007/978-3-642-31395-0_5)
- 789 Join, J.-L., Folio, J.-L., Robineau, B., 2005. Aquifers and groundwater within active shield  
790 volcanoes. Evolution of conceptual models in the Piton de la Fournaise volcano. *J.*  
791
- 792

- 793 Volcanol. Geotherm. Res. 147, 187–201.  
794 <https://doi.org/10.1016/j.jvolgeores.2005.03.013>
- 795 Kluska, J.M., 1997. Evolution magmatique et morpho-structurale du Piton des Neiges au cours  
796 des derniers 500000 ans (Thèse). Université de Paris 11, Orsay.
- 797 Krienitz, M.-S., Garbe-Schönberg, C.-D., Romer, R.L., Meixner, A., Haase, K.M., Stroncik, N.A.,  
798 2012. Lithium Isotope Variations in Ocean Island Basalts—Implications for the  
799 Development of Mantle Heterogeneity. *J. Petrol.* 53, 2333–2347.  
<https://doi.org/10.1093/petrology/egs052>
- 800 Lawrence, R.J., Gedzelman, D.S., 1996. Low stable isotope ratios of tropical cyclone rains.  
801 *Geophys. Res. Lett.* 23, 527–530. <https://doi.org/10.1029/96GL00425>
- 802 Li, L., Bonifacie, M., Aubaud, C., Crispi, O., Dessert, C., Agrinier, P., 2015. Chlorine isotopes of  
803 thermal springs in arc volcanoes for tracing shallow magmatic activity. *Earth Planet. Sci.*  
804 *Lett.* 413, 101–110. <https://doi.org/10.1016/j.epsl.2014.12.044>
- 805 Liu, X.-M., Rudnick, R.L., McDonough, W.F., Cummings, M.L., 2013. Influence of chemical  
806 weathering on the composition of the continental crust: Insights from Li and Nd isotopes  
807 in bauxite profiles developed on Columbia River Basalts. *Geochim. Cosmochim. Acta* 115,  
808 73–91. <https://doi.org/10.1016/j.gca.2013.03.043>
- 809 Liu, X.-M., Wanner, C., Rudnick, R.L., McDonough, W.F., 2015. Processes controlling  $\delta$ Li in  
810 rivers illuminated by study of streams and groundwaters draining basalts. *Earth Planet.*  
811 *Sci. Lett.* 409, 212–224. <https://doi.org/10.1016/j.epsl.2014.10.032>
- 812 Liuzzo, M., Di Muro, A., Giudice, G., Michon, L., Ferrazzini, V., Gurrieri, S., 2015. New evidence of  
813 CO<sub>2</sub> soil degassing anomalies on Piton de la Fournaise volcano and the link with volcano  
814 tectonic structures. *Geochem. Geophys. Geosystems* 16, 4388–4404.  
<https://doi.org/10.1002/2015GC006032>
- 815 Lopoukhine, M., Stieljes, L., 1978. Evaluation du Potentiel géothermique de l'Île de la Réunion -  
816 1ère Phase exploratoire : Géologie et géochimie des eaux (No. 78 SGN 467 GTH). BRGM.
- 817 Louvat, P., Allègre, C.J., 1997. Present denudation rates on the island of Réunion determined by  
818 river geochemistry: Basalt weathering and mass budget between chemical and  
819 mechanical erosions. *Geochim. Cosmochim. Acta* 61, 3645–3669.  
[https://doi.org/10.1016/S0016-7037\(97\)00180-4](https://doi.org/10.1016/S0016-7037(97)00180-4)
- 820 Marty, B., Meynier, V., Nicolini, E., Griesshaber, E., Toutain, J.P., 1993. Geochemistry of gas  
821 emanations: A case study of the Réunion Hot Spot, Indian Ocean. *Appl. Geochem.* 8,  
822 141–152. [https://doi.org/10.1016/0883-2927\(93\)90030-K](https://doi.org/10.1016/0883-2927(93)90030-K)
- 823 McDougall, I., 1971. The geochronology and evolution of the young volcanic island of Réunion,  
824 Indian Ocean. *Geochim. Cosmochim. Acta* 35, 261–288. [https://doi.org/10.1016/0016-7037\(71\)90037-8](https://doi.org/10.1016/0016-7037(71)90037-8)
- 825 Millot, R., Guerrot, C., Vigier, N., 2004. Accurate and High-Precision Measurement of Lithium  
826 Isotopes in Two Reference Materials by MC-ICP-MS. *Geostand. Geoanalytical Res.* 28,  
827 153–159. <https://doi.org/10.1111/j.1751-908X.2004.tb01052.x>
- 828 Nauret, F., Famin, V., Vlastélic, I., Gannoun, A., 2019. A trace of recycled continental crust in the  
829 Réunion hotspot. *Chem. Geol.* 524, 67–76.  
<https://doi.org/10.1016/j.chemgeo.2019.06.009>
- 830 Nicolini, E., Coudray, J., Grunberger, O., Jusserand, C., 1998. Seasonnal variations in isotopic  
831 content (18O-2H) of rainfall over an intertropical humid island (Reunion Island, southwest  
832 Indian Ocean). *IAHS* 253.
- 833 Nicolini, E., Jusserand, C., Blavoux, B., Coudray, J., Eberschweiler, C., Mairine, P., Aubouin, J.,  
834 1989. Appauvrissement en isotopes lourds des précipitations liées aux cyclones. *Comptes  
835 Rendues Académie Sci.* 309, 1255–1260.
- 836 Nicolini, E., Olive, P., Coudray, J., Jusserand, C., 1991. Circulation des eaux dans le massif du  
837 Piton de la Fournaise (Ile de la Réunion) et leur contamination par des fluides d'origine  
838 magmatique. *Comptes Rendues Académie Sci.* 312, 535–542.
- 839 Panichi, C., Gonfiantini, R., 1981. Geothermal waters. In *Stable Isotope Hydrology*, Technical  
840 Reports Series. INTERNATIONAL ATOMIC ENERGY AGENCY, Vienna.
- 841 Panichi, C., Gonfiantini, R., 1977. Environmental isotopes in geothermal studies. *Geothermics* 6,  
842 143–161. [https://doi.org/10.1016/0375-6505\(77\)90024-4](https://doi.org/10.1016/0375-6505(77)90024-4)

- 848 Peltier, A., Famin, V., Bachèlery, P., Cayol, V., Fukushima, Y., Staudacher, T., 2008. Cyclic  
849 magma storages and transfers at Piton de La Fournaise volcano (La Réunion hotspot)  
850 inferred from deformation and geochemical data. *Earth Planet. Sci. Lett.* 270, 180–188.  
851 <https://doi.org/10.1016/j.epsl.2008.02.042>
- 852 Petit, V., Aunay, B., Gourcy, L., Baran, N., Oliva, Z., Lucas, C., 2013a. Pollution diffuse et  
853 transferts des produits phytosanitaires du sol vers les ressources en eau souterraines de  
854 l'île de La Réunion. (No. RP-61477-FR <http://infoterre.brgm.fr/rapports//RP-61477-FR.pdf>). BRGM.
- 855 Petit, V., Dewandel, B., Charlier, J.B., Ollivier, P., Lucas, C., Oliva, Z., 2013b. Amélioration de la  
856 connaissance hydrogéologique de l'aquifère côtier du Gol. (No. RP-61834-FR  
857 <http://infoterre.brgm.fr/rapports//RP-61834-FR.pdf>). BRGM.
- 858 Pogge von Strandmann, P.A.E., Opfergelt, S., Lai, Y.-J., Sigfússon, B., Gislason, S.R., Burton,  
859 K.W., 2012. Lithium, magnesium and silicon isotope behaviour accompanying weathering  
860 in a basaltic soil and pore water profile in Iceland. *Earth Planet. Sci. Lett.* 339–340, 11–  
861 23. <https://doi.org/10.1016/j.epsl.2012.05.035>
- 862 Rançon, J.P., 1985. Hydrothermal history of Piton des Neiges volcano (Reunion Island, Indian  
863 Ocean). *J. Volcanol. Geotherm. Res.* 26, 297–315. [https://doi.org/10.1016/0377-0273\(85\)90061-7](https://doi.org/10.1016/0377-0273(85)90061-7)
- 864 Rançon, J.P., Rocher, P., 1985. Découverte de zones fumeroliennes récentes dans le cirque de  
865 Salazie (île de La Réunion, Océan Indien). *C R Académie Sci. Sér. II* 16, 821–826.
- 866 Rocher, P., 1988. Contexte volcanique et structural de l'hydrothermalisme récent dans le massif  
867 du Piton des neiges (île de La Réunion): étude détaillée du cirque de Salazie (thesis).  
868 Paris 11.
- 869 Rogers, K.M., Nicolini, E., Gauthier, V., 2012. Identifying source and formation altitudes of  
870 nitrates in drinking water from Réunion Island, France, using a multi-isotopic approach. *J.*  
871 *Contam. Hydrol.* 138–139, 93–103. <https://doi.org/10.1016/j.jconhyd.2012.07.002>
- 872 Ruzié, L., Aubaud, C., Moreira, M., Agrinier, P., Dessert, C., Gréau, C., Crispi, O., 2013. Carbon  
873 and helium isotopes in thermal springs of La Soufrière volcano (Guadeloupe, Lesser  
874 Antilles): Implications for volcanological monitoring. *Chem. Geol.* 359, 70–80.  
875 <https://doi.org/10.1016/j.chemgeo.2013.09.008>
- 876 Ryu, J.-S., Vigier, N., Lee, S.-W., Lee, K.-S., Chadwick, O.A., 2014. Variation of lithium isotope  
877 geochemistry during basalt weathering and secondary mineral transformations in Hawaii.  
878 *Geochim. Cosmochim. Acta* 145, 103–115. <https://doi.org/10.1016/j.gca.2014.08.030>
- 879 Sanjuan, B., Genter, A., Brach, M., Lebon, D., 2001. Compléments d'étude géothermique dans  
880 l'île de la Réunion (géologie, géochimie) (No. RP-51189-FR  
881 (<http://infoterre.brgm.fr/rapports/RP-51189-FR.pdf>)). BRGM.
- 882 Sanjuan, B., Lasne, E., Brach, M., Vaute, L., 1999. Bouillante geothermal field (Guadeloupe).  
883 Geochemical monitoring during the simulation operation. Critical evaluation of chemical  
884 and isotopic field data. (No. RR-40646-FR <http://infoterre.brgm.fr/rapports//RR-40646-FR.pdf>). BRGM.
- 885 Schiffman, P., Watters, R.J., Thompson, N., Walton, A.W., 2006. Hyaloclastites and the slope  
886 stability of Hawaiian volcanoes: Insights from the Hawaiian Scientific Drilling Project's 3-  
887 km drill core. *J. Volcanol. Geotherm. Res., Growth and Collapse of Hawaiian Volcanoes*  
888 151, 217–228. <https://doi.org/10.1016/j.jvolgeores.2005.07.030>
- 889 Smietana, M., 2011. Petrology, geochronology (K-Ar) and elemental and isotopic geochemistry  
890 (Sr, Nd, Hf, Pb) of older lavas of Reunion: Implications for the construction of the  
891 volcanic edifice (Theses). Université de la Réunion.
- 892 Sveinbjörnsdóttir, A.E., Coleman, M.L., Yardley, B.W.D., 1986. Origin and history of hydrothermal  
893 fluids of the Reykjanes and Krafla geothermal fields, Iceland. *Contrib. Mineral. Petrol.* 94,  
894 99–109. <https://doi.org/10.1007/BF00371231>
- 895 Tello, H., Verma, M.P., Tovar, A., 2000. Origin of acidity in the Los Humeros, Mexico, geothermal  
896 reservoir, in: Proceedings World Geothermal Congress, Japan. pp. 2959–2966.
- 897 Thomas, D.M., 1984. Geothermal resources assessment in Hawaii. Final report (No.  
898 DOE/SF/10819-T1). Hawaii Univ., Honolulu (USA). Hawaii Inst. of Geophysics.  
899 <https://doi.org/10.2172/6761857>

- 903 Trull, T., Nadeau, S., Pineau, F., Polve', M., Javoy, M., 1993. C-He systematics in hotspot  
904 xenoliths: Implications for mantle carbon contents and carbon recycling. *Earth Planet. Sci.*  
905 *Lett.* 118, 43–64. [https://doi.org/10.1016/0012-821X\(93\)90158-6](https://doi.org/10.1016/0012-821X(93)90158-6)
- 906 Vigouroux, N., Williams-Jones, A.E., Wallace, P., Staudacher, T., 2009. The November 2002  
907 eruption of Piton de la Fournaise, Réunion: tracking the pre-eruptive thermal evolution of  
908 magma using melt inclusions. *Bull. Volcanol.* 71, 1077. <https://doi.org/10.1007/s00445-009-0287-5>
- 910 Violette, S., Ledoux, E., Goblet, P., Carbonnel, J.-P., 1997. Hydrologic and thermal modeling of  
911 an active volcano: the Piton de la Fournaise, Reunion. *J. Hydrol.* 191, 37–63.  
912 [https://doi.org/10.1016/S0022-1694\(96\)03071-5](https://doi.org/10.1016/S0022-1694(96)03071-5)
- 913 Vlastélic, I., Menard, G., Gannoun, A., Piro, J.-L., Staudacher, T., Famin, V., 2013. Magma  
914 degassing during the April 2007 collapse of Piton de la Fournaise: The record of semi-  
915 volatile trace elements (Li, B, Cu, In, Sn, Cd, Re, Ti, Bi). *J. Volcanol. Geotherm. Res.* 254,  
916 94–107. <https://doi.org/10.1016/j.jvolgeores.2012.12.027>
- 917 Vlastélic, I., Peltier, A., Staudacher, T., 2007. Short-term (1998–2006) fluctuations of Pb isotopes  
918 at Piton de la Fournaise volcano (Reunion Island): Origins and constraints on the size and  
919 shape of the magma reservoir. *Chem. Geol.* 244, 202–220.  
920 <https://doi.org/10.1016/j.chemgeo.2007.06.015>
- 921 Vlastélic, I., Staudacher, T., Bachèlery, P., Télouk, P., Neuville, D., Benbakkar, M., 2011. Lithium  
922 isotope fractionation during magma degassing: Constraints from silicic differentiates and  
923 natural gas condensates from Piton de la Fournaise volcano (Réunion Island). *Chem.*  
924 *Geol.* <https://doi.org/10.1016/j.chemgeo.2011.02.002>
- 925 Vlastélic, I., Staudacher, T., Semet, M., 2005. Rapid Change of Lava Composition from 1998 to  
926 2002 at Piton de la Fournaise (Réunion) Inferred from Pb Isotopes and Trace Elements:  
927 Evidence for Variable Crustal Contamination. *J. Petrol.* 46, 79–107.  
928 <https://doi.org/10.1093/petrology/egh062>
- 929 Welsch, B., Faure, F., Famin, V., Baronnet, A., Bachèlery, P., 2013. Dendritic Crystallization: A  
930 Single Process for all the Textures of Olivine in Basalts? *J. Petrol.* 54, 539–574.  
931 <https://doi.org/10.1093/petrology/egs077>
- 932

### A. Coordinates of the thermal springs

Table A.1: Coordinates of the thermal springs of Piton des Neiges presented in this study.

Spring	X (UTM, RGR92)	Y (UTM, RGR92)	Elevation (m)
AGS	341428	7669771	1234
BACH	343450	7669284	1011
BB	341878	7660557	931
BC	354418	7665780	720
BE	339734	7662634	919
BR1	340133	7664597	1453
BR10	339242	7663434	1008
BR11	339222	7663287	947
BR12	339338	7663175	932
BR13	339601	7662829	906
BR14	339559	7662782	884
BR15	339465	7662529	840
BR16	339529	7662249	791
BR17	339550	7662153	782
BR18	339567	7662024	777
BR2	339999	7664829	1359
BR21	340184	7665618	1661
BR27	339258	7663521	1008
BR3	339912	7664553	1271
BR4	339782	7664516	1185
BR5	339769	7664504	1190
BR6	339721	7664362	1134
BR7	339529	7664121	1078
BR8	339292	7663643	1022
BR9	339260	7663531	1015
DUP	343744	7669677	892
EDN	344487	7668615	1058
FJ1	338996	7662583	1006
FJ2	338966	7662600	1021
FJ3	339358	7662387	928
G1	338855	7663801	1192
G2	339056	7663709	1091
G3	339051	7663737	1101
G4	339090	7663638	1070
GDS	341479	7669885	1197
IMA	343856	7671080	801
IRN	341149	7662647	1117
MAN	344715	7667560	1313
MAN G	344700	7667550	1317
MANECE	341462	7662815	1241
MF1	335119	7668857	885
OLIV1	344106	7671310	681
OLIV2	343763	7671331	777
OLIVbis	343765	7671332	777
PC	343597	7673440	675
PISSA	339842	7664302	1229
RB1	340894	7669768	1335
RFOUQ	343335	7670620	901
RR1	338790	7661807	722
sRMAT	344434	7671264	652
sRMAT2	343700	7670120	841
sRMAT3	343690	7670160	833
TB	343948	7670835	720
TBA	343696	7670129	834
TR	341983	7674700	905
MANECE	341462	7662815	1241

935

## B. Geochemistry of thermal springs: compilation of data from previous studies

936

Table B.1: Published major elements concentrations, C, O, H, Sr, Li and Cl isotope ratios in thermal springs of Piton des Neiges.

Spring	Campaign	Date	Electrical Conductivity ( $\mu\text{S}/\text{cm}$ )	pH	Temperature (°C)	Ca (mmol/L)	Mg (mmol/L)	Na (mmol/L)	K (mmol/L)	$\text{HCO}_3$ (mmol/L)	$\text{SO}_4$ (mmol/L)	Cl (mmol/L)	$\text{SiO}_2$ (mmol/L)	$\text{CO}_3$ (mmol/L)	NH <sub>4</sub> (mmol/L)	$\text{NO}_2$ (mmol/L)	$\text{NO}_3$ (mmol/L)	$\delta^{13}\text{C}$ (‰ PDB)	$\delta^{18}\text{O}$ (‰ VSMOW)	$\delta\text{D}$ (‰ VSMOW)	$^{87}\text{Sr}/^{86}\text{Sr}$	$\delta^{34}\text{S}_{\text{SO}_4}$ (‰ VCDT)
BACH	Sanjuan et al., 2001	21/10/2000	1540	7.4	19.4	3.6	3.5	5.5	0.2	18.7	0.2	0.1	1.5		b.d.l.	b.d.l.	b.d.l.	-1.1	-6.7	-37.2	0.704300	2.0
BACH	Lopoukhine and Stieljes, 1978	25/06/1978	1120	7.6	25.6	1.2	3.4	4.8	0.2	15.5	0.2	0.1	1.3		b.d.l.	b.d.l.	b.d.l.					
BACH	Aunay et al., 2013	12/03/2013	1087	7.0	25.2	2.7	2.4	3.6	0.1	13.9	0.1	0.1	0.4	b.d.l.								
BB	Sanjuan et al., 2001	24/10/2000	1610	6.7	22.6	4.2	3.4	5.5	0.1	15.4	2.1	0.3	1.9		b.d.l.	b.d.l.	b.d.l.					
BB	Lopoukhine and Stieljes, 1978	20/06/1978	1600		26.3	4.0	3.4	5.8	0.1	15.5	2.1	0.3	1.7		b.d.l.	b.d.l.	b.d.l.					
BC	Lopoukhine and Stieljes, 1978	06/07/1978		6.5	22.7	4.3	14.2	7.7	0.4	45.4	0.3	0.1	1.8		b.d.l.	b.d.l.	b.d.l.					
BE	Frissant et al., 2003	01/07/2003	1187	6.3	22.4	3.6	2.1	1.9	0.1	13.2	0.1	0.1	1.6					b.d.l.				
BR1	Frissant et al., 2003	01/07/2003	1364	7.0	17.3	3.4	1.7	6.8	0.1	16.1	0.1	0.1	1.6					b.d.l.				
BR10	Frissant et al., 2003	01/07/2003	950	6.2	18.7	2.1	1.8	1.5	0.0	10.3	0.1	0.1	1.3					b.d.l.				
BR11	Frissant et al., 2003	01/07/2003	896	7.6	20	2.2	1.7	2.0	0.1	9.9	0.1	0.1	1.4					b.d.l.				
BR12	Louvat and Allègre, 1997	1997		6.4	48	1.9	1.7	13.2	0.3	16.7	2.1		2.5									
BR12	Louvat and Allègre, 1997	1997		6.7	47.5	1.5	1.4	12.6	0.3	15.3	1.8	0.1	2.5									
BR12	Lopoukhine and Stieljes, 1978	20/06/1978	1547	6.7	42	2.0	1.7	10.4	0.3	13.4	1.4	0.7	1.7		b.d.l.	b.d.l.	b.d.l.	2.2	-8.2	-50.5	0.704162	4.8
BR12	Sanjuan et al., 2001	25/10/2000	1430	6.3	36.3	1.6	1.3	10.8	0.3	11.6	2.1	0.6	2.1									
BR12	Frissant et al., 2003	01/07/2003	1233	6.3	32.6	1.9	1.1	6.0	0.1	8.0	1.6	0.4	1.2									
BR13	Frissant et al., 2003	01/07/2003	461	7.7	18.1	0.9	1.1	1.0	0.0	4.6	0.1	0.1	0.7									
BR14	Frissant et al., 2003	01/07/2003	1294	6.8	34.5	2.1	1.5	8.2	0.2	13.2	0.6	0.6	2.0									
BR15	Frissant et al., 2003	01/07/2003	1100	7.0	19.9	1.9	2.3	2.4	0.2	11.5	0.2	0.1	1.1						0.01			
BR16	Frissant et al., 2003	01/07/2003	2560	6.6	32	2.7	2.1	18.4	0.8	23.9	0.4	3.0	2.1									
BR17	Frissant et al., 2003	01/07/2003	1262	6.5	27.5	2.1	1.4	8.6	0.3	12.4	1.2	1.2	1.3									
BR18	Frissant et al., 2003	01/07/2003	656	8.2	23	1.3	0.9	3.0	0.1	6.0	1.0	0.1	0.4									
BR2	Frissant et al., 2003	01/07/2003	1162	8.1	14.5	2.3	1.3	5.4	0.1	9.1	1.7	0.1	0.7		0.03	b.d.l.	b.d.l.					
BR27	Iundt et al., 1992	1992	1095	6.6	20.5	1.4	3.4	5.6	0.7	15.0	0.5	0.1	1.0									
BR3	Frissant et al., 2003	01/07/2003	1000	6.3	23.8	3.1	1.3	2.9	0.1	11.9	0.3	0.1	0.7									
BR4	Frissant et al., 2003	01/07/2003	1156	6.7	16.3	3.3	1.4	1.4	0.1	10.4	0.2	0.1	0.6									
BR5	Frissant et al., 2003	01/07/2003	1022	7.1	22.2	2.6	1.1	4.8	0.1	11.5	0.2	0.1	1.0									
BR6	Frissant et al., 2003	01/07/2003	902	6.2	22.1	2.8	0.8	2.7	0.1	8.9	0.5	0.1	0.8									

Spring	Campaign	Date	Electrical Conductivity ( $\mu\text{s}/\text{cm}$ )	pH	Temperature ( $^{\circ}\text{C}$ )	Ca (mmol/L)	Mg (mmol/L)	Na (mmol/L)	K (mmol/L)	$\text{HCO}_3$ (mmol/L)	$\text{SO}_4$ (mmol/L)	Cl (mmol/L)	$\text{SiO}_2$ (mmol/L)	$\text{CO}_3$ (mmol/L)	NH <sub>4</sub> (mmol/L)	$\text{NO}_2$ (mmol/L)	$\text{NO}_3$ (mmol/L)	$\delta^{13}\text{C}$ (‰ PDB)	$\delta^{18}\text{O}$ (‰ VSMOW)	$\delta\text{D}$ (‰ VSMOW)	$^{87}\text{Sr}/^{86}\text{Sr}$	$\delta^{34}\text{S}_{\text{SO}_4}$ (‰ VCDT)	
BR7	Frissant et al., 2003	01/07/2003	930	6.3	17.7	3.5	0.9	1.7	0.1	8.2	0.7	0.1	0.9			b.d.l.	b.d.l.	b.d.l.	b.d.l.	b.d.l.			
BR8	Frissant et al., 2003	01/07/2003	732	6.9	23.5	2.3	1.1	1.2	0.1	8.0	0.2	0.0	1.1			b.d.l.	b.d.l.	b.d.l.	b.d.l.	b.d.l.			
BR9	Frissant et al., 2003	01/07/2003	1003	6.2	26.2	2.4	1.9	2.3	0.1	10.7	0.2	0.1	1.5			b.d.l.	b.d.l.	b.d.l.	b.d.l.	b.d.l.			
FJ1	Frissant et al., 2003	30/05/2003	1115	6.8	18.1	2.3	1.9	1.5	0.1	9.9	0.1	0.1	0.9			b.d.l.	b.d.l.	b.d.l.	b.d.l.	b.d.l.			
FJ2	Frissant et al., 2003	30/05/2003	1356	6.6	20	3.6	2.6	3.2	0.2	14.7	0.1	0.1	1.5			b.d.l.	b.d.l.	b.d.l.	b.d.l.	b.d.l.			
FJ3	Frissant et al., 2003	30/05/2003	479	6.5	19.6	1.1	1.1	0.3	0.0	4.8	0.1	0.1	0.7			b.d.l.	b.d.l.	b.d.l.	b.d.l.	b.d.l.			
G1	Frissant et al., 2003	29/05/2003	1370	6.9	16.8	3.5	1.8	5.0	0.2	14.4	0.3	0.1	1.2			b.d.l.	b.d.l.	b.d.l.	b.d.l.	b.d.l.			
G2	Frissant et al., 2003	29/05/2003	1312	6.9	15	2.8	2.6	2.7	0.1	13.8	0.1	0.1	1.7			b.d.l.	b.d.l.	b.d.l.	b.d.l.	b.d.l.			
G3	Frissant et al., 2003	29/05/2003	1296	6.6	20.2	3.1	2.4	2.3	0.1	13.6	0.1	0.1	1.8			b.d.l.	b.d.l.	b.d.l.	b.d.l.	b.d.l.			
G4	Frissant et al., 2003	29/05/2003	1405	6.2	21.6	3.1	2.4	3.7	0.2	13.7	0.1	0.1	1.8			b.d.l.	b.d.l.	b.d.l.	b.d.l.	b.d.l.			
GDS	Sanjuan et al., 2001	26/10/2000	6.6	18.6	4.6	2.2	1.3	0.1	8.4	2.9	0.1	0.7		b.d.l.	b.d.l.	b.d.l.	-1.4	-4.9	-23.5	0.704336	3.6		
GDS	Aunay et al., 2013	09/11/2011	1086	6.6	19.5	3.0	2.0	1.3	0.1	9.0	1.5	0.1	0.3	b.d.l.	b.d.l.	b.d.l.	b.d.l.	b.d.l.	b.d.l.				
IMA	Lopoukhine and Steltjes, 1978	20/06/1978	1864	6.7	22.5	2.3	2.0	13.7	0.3	20.1	0.6	1.0	1.1		b.d.l.	b.d.l.	b.d.l.	b.d.l.	b.d.l.	b.d.l.			
IRN	Sanjuan et al., 2001	24/10/2000	2370	6.0	37.8	4.6	4.6	16.1	0.2	31.2	1.1	0.1	2.6		b.d.l.	b.d.l.	b.d.l.	b.d.l.	-8.2	-51.3	0.704169	5.3	
IRN	Louvat and Allègre, 1997	1997		6.5	37.7	4.3	4.2	15.4	0.2	30.9	1.2		2.4										
IRN	Louvat and Allègre, 1997	1997		6.3	37.5	3.0	4.1	17.0	0.2	31.8	0.6	0.1	2.2										
IRN	Lopoukhine and Steltjes, 1978	20/06/1978	2733	6.1	38.5	4.3	4.2	15.9	0.2	31.0	0.9	0.1	2.3		b.d.l.	b.d.l.	b.d.l.	b.d.l.	b.d.l.	b.d.l.			
IRN	Iundt et al., 1992	1992	1953	6.0	36.9	3.2	3.7	14.4	0.2	25.0	1.1	0.2	2.5		b.d.l.	b.d.l.	b.d.l.	b.d.l.	b.d.l.	b.d.l.			
MAN	Sanjuan et al., 2001	19/10/2000	1580	6.6	30.6	4.1	3.4	5.0	0.2	19.2	0.1	0.1	2.0		b.d.l.	b.d.l.	b.d.l.	b.d.l.	3	-7.6	-43.9	0.704282	5.6
MAN	Louvat and Allègre, 1997	1997		6.6	30.2	3.2	2.6	4.0	0.2	15.8	0.0	0.1	1.6										
MAN	Lopoukhine and Steltjes, 1978	24/06/1978	1601	6.2	30.5	3.5	3.2	5.3	0.2	35.6	0.1	0.1	1.8		b.d.l.	b.d.l.	b.d.l.	b.d.l.	b.d.l.	b.d.l.			
MAN	Belle, 2014	01/12/2011	1596	6.4	31.4	3.6	3.1	4.9	0.2	18.8	0.1	0.1	2.0	b.d.l.	b.d.l.	b.d.l.	b.d.l.	-7.3	-45.9	0.704287			
MAN	Aunay et al., 2013	06/03/2012	1369	6.2	31.3	3.2	2.8	4.3	0.2	16.6	0.1	0.1	1.7	b.d.l.	b.d.l.	b.d.l.	b.d.l.	0.02	-6.9	-42.4	0.704277		
MAN G	Sanjuan et al., 2001	19/10/2000	1333	7.9	19	4.0	3.0	2.7	0.1	15.8	0.1	0.0	1.6		b.d.l.	b.d.l.	b.d.l.	b.d.l.	-7.0	-39.8			
MANES	Sanjuan et al., 2001	24/10/2000	2260	5.3	31	4.0	4.1	12.9	0.2	26.7	0.8	0.1	2.1		b.d.l.	b.d.l.	b.d.l.	b.d.l.	3.2	-8.2	-54.3		
MANES	Iundt et al., 1992	1992	1632	6.0	30.1	3.4	3.5	11.4	0.2	22.5	0.7	0.1	2.1		b.d.l.	b.d.l.	b.d.l.	b.d.l.	b.d.l.	b.d.l.			
MF1	Lopoukhine and Steltjes, 1978	29/06/1978	483	9.4	16	0.1	0.0	3.5	0.0	0.3	0.4	2.2	0.9	0.17	b.d.l.	b.d.l.	b.d.l.	b.d.l.	-4.5	-6.5	-40.1		3.0
OLIV1	Sanjuan et al., 2001	01/10/2000	994	7.3	18.9	1.4	1.3	5.7	0.1	8.2	0.5	1.4	0.7		b.d.l.	b.d.l.	b.d.l.	b.d.l.	-4.5	-6.5	-40.1		
OLIV2	Sanjuan et al., 2001	26/10/2000	4980	6.1	26	4.1	4.6	47.0	0.5	42.7	3.2	12.9	0.8		b.d.l.	b.d.l.	b.d.l.	b.d.l.	1.8	-7.8	-45.9	0.704270	8.9
OLIVbis	Aunay et al., 2013	12/02/2013	765	7.6	18.6	2.3	1.4	1.8	0.1	5.5	1.7	0.1	0.3	b.d.l.	b.d.l.	b.d.l.	b.d.l.	0.01					
PC	Aunay et al., 2013	03/09/2012	478	7.3	21.6	1.2	1.1	0.6	0.2	5.0	0.1	0.1	0.8	b.d.l.	b.d.l.	b.d.l.	b.d.l.	0.01	-6.7	-41.4			
PISSA	Sanjuan et al., 2001	26/10/2000	1190	6.7	18.4	4.4	1.4	3.1	0.0	11.6	1.3	0.0	1.3		b.d.l.	b.d.l.	b.d.l.	b.d.l.					

Spring	Campaign	Date	Electrical Conductivity ( $\mu\text{s}/\text{cm}$ )	pH	Temperature ( $^{\circ}\text{C}$ )	Ca (mmol/L)	Mg (mmol/L)	Na (mmol/L)	K (mmol/L)	$\text{HCO}_3$ (mmol/L)	$\text{SO}_4$ (mmol/L)	Cl (mmol/L)	$\text{SiO}_2$ (mmol/L)	$\text{CO}_3$ (mmol/L)	$\text{NH}_4$ (mmol/L)	$\text{NO}_2$ (mmol/L)	$\text{NO}_3$ (mmol/L)	$\delta^{13}\text{C}$ (‰ PDB)	$\delta^{18}\text{O}$ (‰ VSMOW)	$\delta\text{D}$ (‰ VSMOW)	$^{87}\text{Sr}/^{86}\text{Sr}$	$\delta^{34}\text{S}_{\text{SO}_4}$ (‰ VCDT)
RFOUQ	Sanjuan et al., 2001	01/10/2000	1000	7.4	19.2	2.9	2.3	2.2	0.0	11.3	0.3	0.0	0.7	b.d.l.	b.d.l.	b.d.l.	-6.5	-37.9				
RFOUQ	Lopoukhine and Stieljes, 1978	25/06/1978	1418	6.1	22.5	4.1	3.3	3.3	0.1	16.8	0.4	0.1	1.5	b.d.l.	b.d.l.	b.d.l.	-5.9	-36.5				
sRMAT	Sanjuan et al., 2001	01/10/2000	716	7.9	18	1.9	6.0	3.7	0.3	17.7	0.5	0.1	1.2	b.d.l.	b.d.l.	b.d.l.	-6.2	-35.5				
sRMAT2	Sanjuan et al., 2001	21/08/2000	716	7.1	21.2	1.9	1.4	1.9	0.1	8.2	0.1	0.1	0.5	b.d.l.	b.d.l.	b.d.l.						
sRMAT3	Sanjuan et al., 2001	01/10/2000	1380	7.4	26.1	3.5	2.8	9.6	0.2	15.6	2.8	0.3	1.9	0.11	b.d.l.	b.d.l.						
TB	Aunay et al., 2013	01/12/2012	1512	7.0	33.1	1.5	0.7	10.4	0.3	13.9	0.7	0.8	0.9	b.d.l.	b.d.l.	b.d.l.						
TBA	Lopoukhine and Stieljes, 1978	25/06/1978	1752	6.5	27	4.2	2.7	7.2	0.2	17.0	1.8	0.1	1.8	b.d.l.	b.d.l.	b.d.l.						
TBA	Aunay et al., 2013	12/03/2013	1491	6.8	27.2	4.0	2.3	6.1	0.1	16.1	1.4	0.1	1.4	b.d.l.	b.d.l.	b.d.l.						
TR	Belle, 2014	22/11/2011	312	7.1	20.9	0.6	0.6	0.7	0.0	1.3	0.8	0.1	0.5	b.d.l.	b.d.l.	b.d.l.						
TR	Aunay et al., 2013	08/03/2012	1453	6.5	21.2	3.7	4.4	1.2	0.1	0.9	8.3	0.1	0.6	b.d.l.	b.d.l.	b.d.l.	-6.3	-40.3	0.704310		5.8	
VERO	Sanjuan et al., 2001	24/10/2000	2010	5.4	30.3	3.6	3.7	10.9	0.1	23.5	0.7	0.1	2.0	b.d.l.	b.d.l.	b.d.l.	-8.1	-51.2				
VERO	Louvat and Allègre, 1997	1997		6.2	29.6	3.2	3.3	10.4	0.1	22.6	0.7		1.9									
VERO	Louvat and Allègre, 1997	1997		6.2	29.5	3.2	3.2	10.6	0.1	23.9	0.7	0.1	1.9									
VERO	Iundt et al., 1992	1992	1399	6.0	29.2	2.9	3.3	9.4	0.1	19.5	0.6	0.1	1.9	b.d.l.	b.d.l.	b.d.l.						

Table B.2: Trace elements concentrations available in the literature for thermal springs of Piton des Neiges.

Spring	Campaign	Date	Li ( $\mu\text{mol/L}$ )	Be ( $\mu\text{mol/L}$ )	B ( $\mu\text{mol/L}$ )	F (mmol/L)	Al ( $\mu\text{mol/L}$ )	Cr ( $\mu\text{mol/L}$ )	Mn ( $\mu\text{mol/L}$ )	Fe (mmol/L)	Co ( $\mu\text{mol/L}$ )	Ni ( $\mu\text{mol/L}$ )	Cu ( $\mu\text{mol/L}$ )	Zn ( $\mu\text{mol/L}$ )	As ( $\mu\text{mol/L}$ )	Rb ( $\mu\text{mol/L}$ )	Sr ( $\mu\text{mol/L}$ )	Ag ( $\mu\text{mol/L}$ )	Cd ( $\mu\text{mol/L}$ )	Cs ( $\mu\text{mol/L}$ )	Ba ( $\mu\text{mol/L}$ )	Pb ( $\mu\text{mol/L}$ )	U ( $\mu\text{mol/L}$ )	PO4 (mmol/L)
BACH	Sanjuan et al., 2001	21/10/2000	2.88		5.37	b.d.l.	b.d.l.	b.d.l.	b.d.l.	b.d.l.	b.d.l.	0.12	b.d.l.	b.d.l.	0.27	10.39	b.d.l.	b.d.l.	b.d.l.	b.d.l.	b.d.l.	b.d.l.	b.d.l.	b.d.l.0
BACH	Lopoukhine and Stieltjes, 1978	25/06/1978				b.d.l.				b.d.l.						5.71								
BACH	Aunay et al., 2013	12/03/2013																						
BB	Sanjuan et al., 2001	24/10/2000	1.01		10.64	0.01	b.d.l.	b.d.l.	6.61	0.05	0.05	0.75	b.d.l.	b.d.l.	0.06	5.48	b.d.l.	b.d.l.	b.d.l.	b.d.l.	b.d.l.	b.d.l.	b.d.l.0	
BB	Lopoukhine and Stieltjes, 1978	20/06/1978				0.01				0.08						5.71								
BC	Lopoukhine and Stieltjes, 1978	06/07/1978	27.37			0.04				0.03						2.28								
BE	Frissant et al., 2003	01/07/2003				b.d.l.																		
BR1	Frissant et al., 2003	01/07/2003				0.01																		
BR10	Frissant et al., 2003	01/07/2003				0.01																		
BR11	Frissant et al., 2003	01/07/2003				0.01																		
BR12	Louvat and Allègre, 1997	1997	25.36		181.87											1.12	7.61							0.21
BR12	Louvat and Allègre, 1997	1997	26.22													1.04	6.09							0.22
BR12	Lopoukhine and Stieltjes, 1978	20/06/1978	21.61		111.01	0.12				0.01						0.82	7.99							
BR12	Frissant et al., 2003	01/07/2003				0.05																		
BR13	Frissant et al., 2003	01/07/2003				0.01																		
BR14	Sanjuan et al., 2001	25/10/2000	25.64		138.85	0.14	b.d.l.	b.d.l.	2.69	b.d.l.	b.d.l.	b.d.l.	b.d.l.	b.d.l.	b.d.l.	0.94	5.02	b.d.l.	b.d.l.	0.03	0.24	b.d.l.	b.d.l.	b.d.l.0
BR14	Frissant et al., 2003	01/07/2003				0.04																		
BR15	Frissant et al., 2003	01/07/2003				0.01																		
BR16	Frissant et al., 2003	01/07/2003				0.18																		
BR17	Frissant et al., 2003	01/07/2003				0.03																		
BR18	Frissant et al., 2003	01/07/2003				0.01																		
BR2	Frissant et al., 2003	01/07/2003				0.02																		
BR27	Iundt et al., 1992	1992		b.d.l.	17.39	0.02		b.d.l.	7.99	0.04	b.d.l.	b.d.l.	b.d.l.	b.d.l.	b.d.l.		4.45	b.d.l.	b.d.l.	b.d.l.	b.d.l.	b.d.l.	b.d.l.	b.d.l.0
BR3	Frissant et al., 2003	01/07/2003				0.02																		
BR4	Frissant et al., 2003	01/07/2003				0.02																		
BR5	Frissant et al., 2003	01/07/2003				0.01																		
BR6	Frissant et al., 2003	01/07/2003				0.02																		
BR7	Frissant et al., 2003	01/07/2003				0.01																		
BR8	Frissant et al., 2003	01/07/2003				0.02																		
BR9	Frissant et al., 2003	01/07/2003				b.d.l.																		
FJ1	Frissant et al., 2003	30/05/2003				0.02																		

Spring	Campaign	Date	Li ( $\mu\text{mol/L}$ )	Be ( $\mu\text{mol/L}$ )	B ( $\mu\text{mol/L}$ )	F ( $\text{mmol/L}$ )	Al ( $\mu\text{mol/L}$ )	Cr ( $\mu\text{mol/L}$ )	Mn ( $\mu\text{mol/L}$ )	Fe ( $\text{mmol/L}$ )	Co ( $\mu\text{mol/L}$ )	Ni ( $\mu\text{mol/L}$ )	Cu ( $\mu\text{mol/L}$ )	Zn ( $\mu\text{mol/L}$ )	As ( $\mu\text{mol/L}$ )	Rb ( $\mu\text{mol/L}$ )	Sr ( $\mu\text{mol/L}$ )	Ag ( $\mu\text{mol/L}$ )	Cd ( $\mu\text{mol/L}$ )	Cs ( $\mu\text{mol/L}$ )	Ba ( $\mu\text{mol/L}$ )	Pb ( $\mu\text{mol/L}$ )	U ( $\mu\text{mol/L}$ )	PO4 ( $\text{mmol/L}$ )
FJ2	Frissant et al., 2003	30/05/2003				0.01																		
FJ3	Frissant et al., 2003	30/05/2003				0.02																		
G1	Frissant et al., 2003	29/05/2003				0.01																		
G2	Frissant et al., 2003	29/05/2003				0.03																		
G3	Frissant et al., 2003	29/05/2003				0.03																		
G4	Frissant et al., 2003	29/05/2003				0.03																		
GDS	Sanjuan et al., 2001	26/10/2000	0.58		2.04	0.01	b.d.l.	b.d.l.	b.d.l.	b.d.l.	b.d.l.	0.19	b.d.l.	b.d.l.	b.d.l.	0.16	11.18	b.d.l.	b.d.l.	b.d.l.	b.d.l.	b.d.l.	b.d.l.	b.d.l.0
GDS	Aunay et al., 2013	09/11/2011																						
IMA	Lopoukhine and Stieltjes, 1978	20/06/1978	12.97		138.8	0.08						0.01						7.99						
IRN	Sanjuan et al., 2001	24/10/2000	1.44		11.6	b.d.l.	b.d.l.	0.19	8.12	0.16	0.07	1.06	b.d.l.	b.d.l.	b.d.l.	0.60	18.60	b.d.l.	b.d.l.	b.d.l.	0.04	b.d.l.	b.d.l.	b.d.l.0
IRN	Louvat and Allègre, 1997	1997	1.44														0.55	19.25			0.03			
IRN	Louvat and Allègre, 1997	1997	1.58		8.1												0.55	1.44			b.d.l.			
IRN	Lopoukhine and Stieltjes, 1978	20/06/1978			18.5	b.d.l.						0.13					0.94	20.54						
IRN	Iundt et al., 1992	1992		b.d.l.	14.2	b.d.l.	b.d.l.	8.28	0.12	b.d.l.	b.d.l.	b.d.l.	b.d.l.	b.d.l.	0.30	6.51	b.d.l.	b.d.l.	b.d.l.	b.d.l.	b.d.l.	b.d.l.	b.d.l.0	
MAN	Sanjuan et al., 2001	19/10/2000	4.75		7.9	0.01	b.d.l.	0.10	13.11	0.06	0.03	0.49	b.d.l.	b.d.l.	b.d.l.	0.23	9.13	b.d.l.	b.d.l.	b.d.l.	0.18	b.d.l.	b.d.l.	b.d.l.0
MAN	Louvat and Allègre, 1997	1997	4.03			0.01						0.06					7.95				0.13			
MAN	Lopoukhine and Stieltjes, 1978	24/06/1978	4.32														10.27							
MAN	Belle, 2014	01/12/2011			4.2		0.06		16.18	0.07							9.28							
MAN	Aunay et al., 2013	06/03/2012															7.91							
MAN G	Sanjuan et al., 2001	19/10/2000	2.16		4.6	b.d.l.	1.48	b.d.l.	8.85	b.d.l.	0.03	0.41	b.d.l.	b.d.l.	b.d.l.	0.47	10.16	b.d.l.	b.d.l.	0.06	b.d.l.	b.d.l.	b.d.l.0	
MANES	Sanjuan et al., 2001	24/10/2000	1.01		9.3	b.d.l.	b.d.l.	0.17	9.01	0.13	0.07	1.02	b.d.l.	b.d.l.	b.d.l.	0.47	15.64	b.d.l.	b.d.l.	b.d.l.	b.d.l.	b.d.l.	b.d.l.	b.d.l.0
MANES	Iundt et al., 1992	1992		b.d.l.	10.5	b.d.l.	b.d.l.	8.92	0.11	b.d.l.	b.d.l.	b.d.l.	b.d.l.	b.d.l.			13.58	b.d.l.	b.d.l.	b.d.l.	b.d.l.	b.d.l.	b.d.l.	b.d.l.0
MF1	Lopoukhine and Stieltjes, 1978	29/06/1978			0.02						0.03													
OLIV1	Sanjuan et al., 2001	01/10/2000	3.17		152.5	0.02	b.d.l.	b.d.l.	0.49	b.d.l.	b.d.l.	b.d.l.	b.d.l.	b.d.l.	b.d.l.	0.82	2.62	b.d.l.	b.d.l.	b.d.l.	b.d.l.	b.d.l.	b.d.l.	b.d.l.0
OLIV2	Sanjuan et al., 2001	26/10/2000	5.91		1992	0.04	2.97	0.62	5.70	0.01	b.d.l.	0.17	b.d.l.	b.d.l.	b.d.l.	0.82	19.86	b.d.l.	b.d.l.	b.d.l.	0.06	b.d.l.	0.01	b.d.l.0
OLIVbis	Aunay et al., 2013	12/02/2013																						
PC	Aunay et al., 2013	03/09/2012																						
PISSA	Sanjuan et al., 2001	26/10/2000	0.43		6.8	b.d.l.	b.d.l.	b.d.l.	8.86	0.04	b.d.l.	0.29	b.d.l.	b.d.l.	b.d.l.		28.42	b.d.l.	b.d.l.	b.d.l.	b.d.l.	b.d.l.	b.d.l.	b.d.l.0
RFOUQ	Sanjuan et al., 2001	01/10/2000	b.d.l.		0.0	b.d.l.	b.d.l.	b.d.l.	b.d.l.	b.d.l.	b.d.l.	b.d.l.	b.d.l.	b.d.l.	b.d.l.		7.30	b.d.l.	b.d.l.	b.d.l.	b.d.l.	b.d.l.	b.d.l.	b.d.l.0
RFOUQ	Lopoukhine and Stieltjes, 1978	25/06/1978				0.01					0.06						10.27							
sRMAT	Sanjuan et al., 2001	01/10/2000	3.75		7.3	0.01	b.d.l.	b.d.l.	0.42	b.d.l.	b.d.l.	b.d.l.	b.d.l.	b.d.l.	b.d.l.		6.05	b.d.l.	b.d.l.	0.06	b.d.l.	b.d.l.	b.d.l.	b.d.l.0
sRMAT2	Sanjuan et al., 2001	21/08/2000	0.14		b.d.l.	b.d.l.	b.d.l.	b.d.l.	0.25	b.d.l.	b.d.l.	0.10	b.d.l.	b.d.l.	b.d.l.		6.51	b.d.l.	b.d.l.	b.d.l.	b.d.l.	b.d.l.	b.d.l.	b.d.l.0
sRMAT3	Sanjuan et al., 2001	01/10/2000	1.44		7.0	0.01	1.11	b.d.l.	2.95	0.01	0.05	0.22	0.05	b.d.l.	b.d.l.		8.22	b.d.l.	b.d.l.	0.09	b.d.l.	b.d.l.	b.d.l.	b.d.l.0

Spring	Campaign	Date	Li ( $\mu\text{mol/L}$ )	Be ( $\mu\text{mol/L}$ )	B ( $\mu\text{mol/L}$ )	F (mmol/L)	Al ( $\mu\text{mol/L}$ )	Cr ( $\mu\text{mol/L}$ )	Mn ( $\mu\text{mol/L}$ )	Fe (mmol/L)	Co ( $\mu\text{mol/L}$ )	Ni ( $\mu\text{mol/L}$ )	Cu ( $\mu\text{mol/L}$ )	Zn ( $\mu\text{mol/L}$ )	As ( $\mu\text{mol/L}$ )	Rb ( $\mu\text{mol/L}$ )	Sr ( $\mu\text{mol/L}$ )	Ag ( $\mu\text{mol/L}$ )	Cd ( $\mu\text{mol/L}$ )	Cs ( $\mu\text{mol/L}$ )	Ba ( $\mu\text{mol/L}$ )	Pb ( $\mu\text{mol/L}$ )	U ( $\mu\text{mol/L}$ )	PO4 (mmol/L)
TB	Aunay et al., 2013	01/12/2012																						
TBA	Lopoukhine and Stieltjes, 1978	25/06/1978				0.02				0.06						11.41								
TBA	Aunay et al., 2013	12/03/2013																						
TR	Belle, 2014	22/11/2011						0.21		1.71	0.01						1.34							
TR	Aunay et al., 2013	08/03/2012															7.89							
VERO	Sanjuan et al., 2001	24/10/2000	0.86		7.9	b.d.l.	b.d.l.	0.15	7.17	0.11	0.05	0.95	b.d.l.	0.12	b.d.l.	0.54	14.15	b.d.l.	b.d.l.	b.d.l.	b.d.l.	b.d.l.	b.d.l.	b.d.l.0
VERO	Louvat and Allègre, 1997	1997	0.86													0.39	14.20							
VERO	Louvat and Allègre, 1997	1997	1.01		0.6	b.d.l.	b.d.l.	b.d.l.	6.55	0.08	b.d.l.	b.d.l.	b.d.l.	b.d.l.	b.d.l.	0.39	5.80							
VERO	Iundt et al., 1992	1992		b.d.l.	7.9	b.d.l.	b.d.l.	b.d.l.									9.24	b.d.l.	b.d.l.	b.d.l.	b.d.l.	b.d.l.	b.d.l.	b.d.l.0

939

940

Table B.3: Literature carbon speciation and isotopic ratios in waters and gas from thermal springs of Piton des Neiges.

Spring	Source of data	pH	Temperature (°C)	TDIC (mmol/L)	H <sub>2</sub> CO <sub>3</sub> (mmol/L)	HCO <sub>3</sub> (mmol/L)	$\delta^{13}\text{C}_{\text{TDIC}} (\text{\textperthousand PDB})$	$\delta^{13}\text{C}_{\text{CO}_2} (\text{\textperthousand PDB})$
BACH	Marty et al., 1992	7.77	25.1	14.20	0.46	13.70	2.10	
BACH	Sanjuan et al., 2001	7.42	19.4	20.30	1.59	18.70	-1.10	
BB	Marty et al., 1992	7.22	27.6	23.09	2.29	20.80		-5.8
BB	Sanjuan et al., 2001	6.66	22.6	22.98	7.56	15.43	2.70	
BC	Marty et al., 1992	6.16	26.4	99.17	53.97	45.20		
BR14	Sanjuan et al., 2001	6.32	36.3	24.01	12.42	11.59	2.20	
GDS	Sanjuan et al., 2001	6.57	18.6	13.48	5.07	8.41	-1.40	
IRN	Marty et al., 1992	6.15	38.4	57.61	24.80	32.80	-2.30	-5.8
MAN	Marty et al., 1992	6.02	30.3	44.42	26.42	18.00		-6.7
MAN	Sanjuan et al., 2001	6.59	30.6	30.27	11.06	19.21	3.00	
MANES	Marty et al., 1992	6	31.3	64.59	38.59	26.00	-3.30	-6.3
MANES	Sanjuan et al., 2001	5.3	31	283.66	257.00	26.66	3.2000	
OLIV1	Sanjuan et al., 2001	7.26	18.9	9.21	1.01	8.20	-4.50	
OLIV2	Sanjuan et al., 2001	6.05	26	127.81	85.14	42.67	1.80	
VERO	Marty et al., 1992	6	31.6	58.97	35.07	23.90	-4.20	-6.5

941

942

### C. Detail of water samples of the study area potentially depleted in heavy isotopes of oxygen and hydrogen.

943

Table C.1: Literature oxygen and hydrogen isotopic ratios ( $\text{\textperthousand}$  VSMOW) for water samples used in Figure 3, collected at altitudes > 2000 m and/or associated with a cyclonic event.

Sample	Nature	Source of data	Associated with a cyclonic event	Altitude (m)	Symbol	Date	$\delta^{18}\text{O}$ ( $\text{\textperthousand}$ VSMOW)	$\delta\text{D}$ ( $\text{\textperthousand}$ VSMOW)
Pluie Maido	Rain	Grünberger, 1989	No	2190	+	Dry season 1986	-5.4	-28.7
Pluie Maido	Rain	Grünberger, 1989	No	2190	+	Rainy season 1985-1986	-7.6	-47.0
Pluie Rivière de l'Est Haut	Rain	Nicolini, 1991	No	2250	+	1/4/1985-23/10/1985	-5.3	-19.0
Pluie Rivière de l'Est Haut	Rain	Nicolini, 1991	No	2250	+	23/10/1985-11/4/1986	-7.1	-41.3
Pluie Rivière de l'Est Haut	Rain	Nicolini, 1991	No	2250	+	11/4/1986-10/11/1986	-6.3	-32.6
Pluie Rivière de l'Est Haut	Rain	Nicolini, 1991	Yes	2250	●	10/11/1986-2/4/1987	-11.8	-78.0
Pluie Rivière de l'Est Haut	Rain	Nicolini, 1991	No	2250	+	2/4/1987-29/4/1987	-8.1	-46.1
Pluie Rivière de l'Est Haut	Rain	Nicolini, 1991	No	2250	+	29/4/1987-24/6/1987	-6.1	-29.4
Pluie Rivière de l'Est Haut	Rain	Nicolini, 1991	No	2250	+	24/6/1987-14/8/1987	-6.2	-29.6
Pluie Rivière de l'Est Haut	Rain	Nicolini, 1991	No	2250	+	14/8/1987-23/9/1987	-4.1	-14.2
Eau souterraine Le Blanchard (Trois-Bassins)	Groundwater	Aunay and Gourcy, 2007	Yes	161	✗	08/03/2007	-7.7	-47.5
Ravine Trois-Bassins - RD9	Rain	Aunay and Gourcy, 2007	Yes	368	✗	08/03/2007	-8.5	-57.8

944